Finance and Economics Discussion Series

Federal Reserve Board, Washington, D.C.
ISSN 1936-2854 (Print)
ISSN 2767-3898 (Online)

Beyond the Unemployment Rate: A Structural Labor Market Indicator

Isabel Cairo, Hess Chung, Francesco Ferrante, Cristina Fuentes-Albero, Camilo Morales-Jimenez, Damjan Pfajfar

2026-058

Please cite this paper as:
Cairo, Isabel, Hess Chung, Francesco Ferrante, Cristina Fuentes-Albero, Camilo Morales-Jimenez, and Damjan Pfajfar (2026). "Beyond the Unemployment Rate: A Structural Labor Market Indicator," Finance and Economics Discussion Series 2026-058. Washington: Board of Governors of the Federal Reserve System, https://doi.org/10.17016/FEDS.2026.058.

Beyond the Unemployment Rate: A Structural Labor Market Indicator*

Isabel Cairó[‡] Hess Chung[‡] Francesco Ferrante[‡] Cristina Fuentes-Albero[‡]
Camilo Morales-Jiménez[‡] Damjan Pfajfar[§]

July 2026

Abstract

Labor market variables frequently send conflicting signals about the degree of slack or tightness, often complicating policy assessments at critical junctures. This paper develops a Structural Labor Market Indicator (SLMI) for the U.S. economy that addresses the limitations of existing univariate measures or atheoretical statistical approaches that synthesize multiple labor market indicators but cannot distinguish between supply and demand driving forces. We construct the SLMI using a medium-scale New Keynesian DSGE model featuring search and matching frictions, endogenous labor force participation, and variable hours. The model is disciplined by a comprehensive dataset that includes not only labor market variables but also other macroeconomic aggregates. The SLMI synthesizes model-implied gaps across multiple labor market dimensions using principal component analysis. We show that GDP growth and inflation provide substantial information about labor market slack beyond what labor market variables contain, validating our multi-variable structural approach. Relative to alternative measures, the SLMI often provides earlier warnings of deteriorating conditions at recession onset but recovers more gradually during expansions.

JEL Classification: E32, J64, J20, E37.
Keywords: Search and matching, labor market, labor market slack.

*The views expressed in this paper are solely the responsibility of the authors and should not be interpreted as reflecting the views of the Board of Governors of the Federal Reserve System, Federal Reserve Bank of Cleveland, or of anyone else associated with the Federal Reserve System.

[‡] *Address:* Board of Governors of the Federal Reserve System, 20th Street and Constitution Avenue NW, Washington, D.C. 20551, USA *Email addresses*: isabel.cairo@frb.gov (I. Cairó), hess.t.chung@frb.gov (H. Chung), francesco.ferrante@frb.gov (F. Ferrante), cristina.fuentes-albero@frb.gov (C. Fuentes-Albero), camilo.moralesjimenez@frb.gov (C. Morales-Jiménez).

[§] *Address:* Federal Reserve Bank of Cleveland, 1455 E 6th Str., Cleveland, OH 44114, USA. *Email address*: damjan.pfajfar@clev.frb.org (D. Pfajfar).

1 Introduction

The labor market often confronts policymakers with conflicting signals about labor market slack, complicating the assessment of appropriate policy. For example, in December 2015, the unemployment rate had fallen to 5 percent, near most contemporary estimates of full employment, yet participation had declined nearly two percentage points since the recovery began, and nominal wage growth remained below 3 percent, short of levels consistent with a tight labor market. In 2021-2022, unemployment returned to its pre-pandemic level of roughly 4 percent even as the vacancy-to-unemployment ratio exceeded 2 and average weekly hours sat below trend. The puzzle is again live today: through 2025-2026 unemployment has hovered around 4 percent while vacancies have fallen sharply from their post-pandemic peaks, leaving open whether labor markets are genuinely loosening or whether the earlier vacancy surge reflected transitory post-pandemic distortions rather than true tightness. These episodes share a common feature: labor market indicators disagree, and the cost of misreading the underlying slack is high for policymakers. This paper develops a structural approach to synthesizing information across labor market margins, alongside key macroeconomic aggregates, into a single model-consistent measure of slack.

Measuring slack is a difficult task that extends beyond simply observing conflicting indicators in a dashboard; it is a conceptual and identification problem. Labor supply and demand adjust along multiple margins simultaneously: extensive (employment, unemployment, participation), intensive (hours per worker), vacancy posting, and wage determination. No single indicator captures this multi-dimensionality. Unemployment abstracts from participation and hours; the vacancy-to-unemployment ratio, though informative about tightness, omits employed workers' desired hours; wage growth conflates supply and demand shifts, making it an ambiguous signal of slack absent further structure. Even observing every margin presents three key challenges. First, how to aggregate this multidimensional information? Second, should the assessment draw on labor data alone, or do other aggregates signal whether labor resources are fully utilized? For instance, strong GDP growth with subdued inflation suggest slack at a given unemployment rate, while weak growth and elevated inflation suggest tightness. Third, the source of fluctuations matters: unemployment driven by adverse supply shocks calls for a different monetary policy response than unemployment driven by deficient aggregate demand. A dashboard of indicators read through subjective judgment offers no systematic way to confront aggregation, information extraction, or identification, leaving policymakers without guidance precisely when labor markets are most confounding.

We address these challenges by constructing a Structural Labor Market Slack (SLMI) indicator grounded in a medium-scale New Keynesian DSGE model with search and matching frictions, endogenous labor force participation, and variable hours worked, featuring nominal price and wage rigidities. The model builds on Cairó et al. (2026), which we extend by introducing wealth into household utility. This form of the utility function decouples the steady-state federal funds rate from longer-run real GDP growth, as observed in the data. Defining slack by comparing actual outcomes relative to their flexible-price-and-wage equilibrium counterparts, we compute model-implied gaps for nine labor market variables—employment, unemployment (both the rate and level), labor force participation, total hours, average workweek, vacancies, labor market tightness, and real wages—and extract their common cyclical component via principal component analysis. We label that component the SLMI. Because the model is estimated on a comprehensive dataset spanning not only labor market variables but also aggregate output, consumption, investment, inflation, interest rates, and credit spreads, the gaps inherit information from broader macroeconomic conditions, and the structural framework is better able to identify the supply and demand disturbances behind labor market fluctuations. We validate the model against U.S. data from 1987–2026, showing that it reproduces key cyclical movements and, in particular, the dynamic co-movements and lead-lag relationships among labor market and macro variables observed in the data.

Our analysis yields two interesting findings. First, and relative to alternative slack measures, the SLMI often displays distinct cyclical behavior at business cycle turning points. It tends to warn earlier of deterioration at recession onset and recover more slowly thereafter, though the magnitude and timing of these differences vary across episodes. Second, decomposing the SLMI reveals that GDP growth and inflation carry substantial information about slack beyond what labor variables alone contain, underscoring that slack needs to be judged in conjunction with the broader macroeconomic context. Historical shock decompositions attribute the bulk of SLMI variation over the 1987–2026 period to risk premium and investment efficiency shocks, which drove the deep slack of 2008–2009 financial crisis and the COVID-19 recession; monetary policy shocks play only a modest role and become negligible after 2013 once we allow time-varying Taylor rule coefficients.

This paper makes three important contributions. First, we provide the first structural labor market indicator that synthesizes all major labor market margins—employment, participation, hours, vacancies, and wages—within a disciplined DSGE model rather than a purely statistical aggregation. The structural discipline pays off: the first principle component of our model-implied gaps explains the vast majority of total variance and it is the only component with an eigenvalue above one, whereas applying PCA directly to filtered labor market data yields up to three such components, providing a diffuse factor structure that obscures the underlying signal. Because the SLMI also draws on output, consumption, investment, inflation, interest rates, and credit spreads, it can read the same unemployment rate as more or less slack depending on the macroeconomic context, and it can separate supply from demand disturbances, support counterfactual experiments, and be decomposed into contributions from specific shocks and observables—none of which is available to approaches built on labor market alone. Second, we incorporate time-varying monetary policy rule coefficients estimate from the Federal Open Market Committee's (FOMC) Summary of Economic Projections (SEP) by González-Astudillo and Tanvir (2026), preventing attributing systematic shifts in monetary policy making to policy shocks, which would distort our inference about labor market slack. Third, we offer a practical tool for real-time analysis with formal uncertainty quantification: credible intervals constructed via Monte Carlo simulation over the parameter distribution, which reveal that uncertainty about slack is especially elevated during recoveries. Note that these results are model dependent, resting on judgments about structural features, long-run calibration, and shock specification. However, we show that the model successfully reproduces key U.S. business cycle properties and generates output and unemployment rate gaps broadly consistent with external estimates.

This paper contributes to a large literature on measuring unobservable economic slack and natural rates. The output gap has been estimated with univariate filters, production function approaches that aggregate factor-utilization estimates (Congressional Budget Office, 2026; Kiley, 2013), and multivariate filters exploiting the output-inflation correlation (Blagrave et al., 2015); the natural rate of unemployment with time-varying parameter methods (Staiger et al., 1997; Gordon, 1997), with attention to surrounding (Orphanides and Williams, 2002); and the natural rate of interest with frameworks emphasizing that equilibrium concepts themselves drift with structural change (Laubach and Williams, 2003; Holston et al., 2017). Most of this work, however, treats single-variable gaps and is silent on synthesizing information across labor market margins. Chung et al. (2014) and Hakkio and Willis (2014) take a step in that direction by applying principal component analysis to labor market indicators, but a purely statistical summary of co-movement cannot distinguish supply from demand, offers no route to incorporate non-labor data, and supports no counterfactual or shock decomposition. We also build on work studying endogenous labor supply along the extensive (e.g. Cairó et al., 2022, Krusell et al., 2017, 2020, Campolmi and Gnocchi, 2016 and Nucci and Riggi, 2018) and intensive (e.g. Cacciatore et al., 2020) margins, and how it shapes cyclical labor market dynamics (e.g. Elsby et al., 2015, Christiano et al., 2015 and Christiano et al., 2021).

The remainder of the paper proceeds as follows: Section 2 describes the model structure and calibration strategy; Section 3 validates the model's ability to match U.S. business cycle properties; Section 4 constructs the SLMI and examines its historical evolution; Section 5 compares the SLMI to alternative slack measures; and Section 6 quantifies uncertainty around the indicator and compares the two-sided with the one-sided filtered indicator, more suitable for practical policy analysis. Finally, Section 7 concludes.

2 Model Description and Calibration

We adopt the medium-scale New Keynesian model of Cairó et al. (2026) as our baseline framework. The Cairó et al. (2026) model incorporates search and matching frictions alongside endogenous labor force participation and hours worked decisions. Therefore, this model includes the multiple margins of adjustment that a comprehensive labor market indicator must capture. We then introduce three targeted modifications to adopt their framework to our purposes: *(i)* we augment household preferences with a wealth-in-the-utility term that decouples the steady-state real interest rate from longer-run GDP growth; *(ii)* we update the calibration of longer-run values to reflect the most recent assessments from the Congressional Budget Office (CBO) and the FOMC's SEP; and *(iii)* we incorporate time-varying coefficients in the monetary policy rule, estimated using median SEP data, to prevent systematic changes in monetary policy from being attributed to monetary policy shocks. This section provides a concise overview of the baseline model, with a particular emphasis on the different labor market margins of adjustment, and then discusses each modification. Detailed model derivations and additional model specifications are provided in Appendix A.

2.1 Baseline Framework

Households

The economy is populated by a representative household with a continuum of members who make labor supply decisions along both the extensive and intensive margins. Each household member can be employed, unemployed and searching for a job, or out of the labor force. The household chooses consumption, bond holdings, labor force participation, and hours worked to maximize expected lifetime utility. Preferences follow Jaimovich and Rebelo (2009) specification, allowing for flexible parameterization of wealth effects on both labor supply margins while maintaining consistency with balanced growth. Perfect consumption insurance across household members ensures that all members consume identical bundles regardless of their employment status, and the household's stochastic discount factor governs all intertemporal decisions.

Production

On the production side, there are five types of firms. A final goods producer purchases differentiated products from retailers and aggregates them into a final consumption good that is sold in a perfectly competitive market. Retailers operate in a monopolistically competitive market and face nominal price rigidities à la Calvo: each period, only a fraction of retailers can re-optimize their prices, while the remainder index their prices to past inflation. Retailers produce using an intermediate good, which they purchase in a perfectly competitive market. Intermediate goods producers operate in a competitive market and produce output using capital and labor via a Cobb-Douglas technology. The labor market is characterized by search and matching frictions: firms post vacancies and match with job searchers according to a standard matching function, and wages are determined through staggered Nash bargaining, which introduces nominal wage rigidities. Hiring is costly, with a generalized recruiting cost function that distinguishes between pre-match costs (vacancy posting) and post-match costs (worker training). Capital is produced by competitive capital producers who face investment adjustment costs. Entrepreneurs purchase capital using a combination of net worth and external finance, and they rent capital services to intermediate goods producers. Following Bernanke et al. (1999), financial frictions arise from a costly state verification problem, generating an endogenous spread between the return on capital and the risk-free rate.

Monetary Policy Rule

Finally, monetary policy follows an inertial Taylor-type rule, with the nominal interest rate responding to deviations of inflation from its target, the output gap, and output gap growth, subject to an effective lower bound constraint.

$$i_t = i_{t-1}^{\rho_i} \left[(R\pi) \left(\frac{\pi_t}{\pi^\star}\right)^{\kappa_\pi} \left(\frac{Y_t}{Y_t^f}\right)^{\kappa_y} \left(\frac{Y_t/{Y_t}^f}{Y_{t-1}/Y_{t-1}^f}\right)^{\kappa_{gy}} \right]^{(1-\rho_i)} \mu_t^m. \tag{1}$$

2.2 Modifications to the Baseline Framework

We calibrate the structural parameters governing preferences, technology, and rigidities at the posterior estimates reported in Cairó et al. (2026) and listed in Appendix A. In Section 3, we show that the baseline parameterization, combined with the three modifications described below, delivers strong empirical performance, closely matching key business cycle moments in the data and producing realistic labor market dynamics across multiple margins.

Wealth in the Utility Function

In the baseline model of Cairó et al. (2026), standard Euler-equation logic ties the steady-state real interest rate to the rate of time preference and the consumption growth rate. While standard in the literature, this tight link is not supported by the data: over recent decades, real interest rates and GDP growth have diverged substantially. To break this connection, we augment the household utility function with a linear wealth term, $\chi_t B_t$, where χ_t grows with technology to guarantee a balanced growth path and B_t represents bond holdings. This modification alters the household's Euler equation, providing an additional degree of freedom that allows the steady-state real interest rate to be calibrated independently of the consumption growth rate. With the wealth-in-utility term, we can set the steady-state federal funds rate to 3.0 percent and GDP growth to 2.0 percent, which is consistent with the FOMC's SEP, without these values being mechanically linked.

Updated Longer-Run Calibration

Table 1 reports the key calibrated parameters that anchor the model's steady state to current assessments of longer-run economic fundamentals. These calibrations are important for ensuring that the model's implications for labor market slack are evaluated relative to a recent empirically plausible longer-run equilibrium. For the steady-state unemployment rate, we calibrate it to 4.3 percent, consistent with the CBO estimates of the natural rate of unemployment based on recent data. The labor force participation rate (LFPR) is set to 61.3 percent, reflecting the structural decline in participation driven by demographic shifts. This value aligns with CBO longer-run projections that account for population aging and changing labor force attachment patterns. Longer-run GDP growth is calibrated to 1.8 percent (annualized), and the federal funds rate to 3.0 percent (annualized), both values consistent with the median longer-run projections from the December 2025 FOMC's SEP. These values capture policymakers' assessments of equilibrium conditions that will prevail once cyclical forces dissipate. We set the persistence parameter of markup shocks to 0.15, reflecting our assessment that markup disturbances in recent years have been relatively short-lived.

Time-Varying Monetary Policy Rule

Our third modification to the model in Cairó et al. (2026) concerns the monetary policy rule. A substantial body of empirical evidence documents significant changes in the conduct of monetary policy over recent

Table 1: Calibrated Parameters and Longer-Run Values

Parameter/Variable	Symbol	Value
Panel A: Longer-run values (in percent)		
Federal funds rate (annualized)	$\bar{i}$	3.0
Unemployment rate	$\bar{u}$	4.3
Labor force participation rate	$\bar{L}$	61.3
GDP growth (annualized)	$\bar{\gamma}$	2.0
Panel B: Structural parameters		
Persistence markup shocks	ρ^{ϵ^p}	0.15

Notes: Long-run steady-state values for the federal funds rate, unemployment rate, labor force participation rate, and GDP growth reflect our assessment of longer-run equilibrium values based on data through 2026.

decades. For example, Clarida et al. (2000) show that the Federal Reserve's systematic response to inflation and output changed markedly between the pre- and post-Volcker periods, while Boivin (2006) and Boivin and Giannoni (2006) provide evidence of evolving policy effectiveness. Primiceri (2005) estimates time-varying coefficients in monetary policy rules using Bayesian methods, finding substantial drift in policy parameters over time. Bauer et al. (2024) estimate meaningful fluctuations in perceived policy rule for monetary policy in the US, in particular over the monetary policy cycle. More recently, González-Astudillo and Tanvir (2026) develop and estimate a forward-guidance Taylor rule with time-varying coefficients showing meaningful fluctuations in the estimated parameters. Beyond this empirical evidence, incorporating time variation in the monetary policy rule is crucial for our analysis because changes in monetary policy, if treated as constant, would be incorrectly attributed to monetary policy shocks. For instance, if the Federal Reserve's response to inflation increased over time but our model assumed a rule with constant parameters, periods of tighter policy due to a systematic higher response to inflation would be interpreted as sequences of contractionary monetary policy shocks. This misspecification would distort our estimates of flexible-price gaps and, consequently, our assessment of labor market slack.

To address this issue, we incorporate time-varying coefficients in the Taylor rule as in González-Astudillo and Tanvir (2026) who estimate them using median SEP projections since 2013. Specifically, three key Taylor rule coefficients are allowed to vary over time: the degree of interest rate smoothing (ρ_i); the response coefficient to inflation deviations from target (κ_π); and the response coefficient to the output gap (κ_y).[1] These time-varying coefficients are treated as known sequences (not subject to uncertainty) when solving the model. Figure A.1 in Appendix A displays the time-varying monetary policy rule coefficients over our sample period. The coefficient on the output gap exhibits remarkable stability, remaining nearly constant throughout the sample, while the inertia parameter shows only minor

[1] González-Astudillo and Tanvir (2026) estimates time-varying Taylor rule coefficients using data from the SEP, which began in 2013. Consequently, the time-varying coefficients in our model apply only from 2013:Q1 onward. Prior to 2013, we use constant coefficients estimated over the pre-2013 sample period. Additionally, beginning in 2013, we set the coefficient on lagged output gap growth (κ_{gy}) to zero, as this term is not included in the analysis by González-Astudillo and Tanvir (2026).

variations over time. In contrast, the coefficient on inflation displays substantial variation, rising to approximately 3.5 in the years preceding the COVID-19 pandemic before gradually declining to around 1.0 by 2025.

We acknowledge that our reliance on SEP data limits the time-varying specification to the post-2013 period. However, we do not view this as a critical limitation for two reasons. First, the constant monetary policy rule estimated for the pre-2013 period captures reasonably well the systematic behavior of Federal Reserve policy during that time, as evidenced by the model's ability to match key moments in the data (see Section 3). Second, as we demonstrate in our historical decompositions below, monetary policy shocks account for a relatively modest share of the variation in flexible-price gaps prior to 2013, suggesting that misspecification of the policy rule during this earlier period would have limited consequences for our estimates of labor market slack.

2.3 Data, Sample Period, and ELB Episodes

We take the model to the data over the period 1987Q1–2025Q4. Because the structural parameters are fixed to the posterior estimates of Cairó et al. (2026) we do not re-estimate the model. Instead, given these parameters and the three modifications described above, we run the Kalman smoother over the full sample to extract the model-implied latent states, including the flexible-price equilibrium counterparts of all labor market variables, from which we construct the gaps that underlie the SLMI. The extended sample encompasses several significant economic episodes beyond the original estimation window: the protracted post-Great-Recession recovery, the COVID-19 pandemic and its aftermath, and the 2021–2023 inflation surge. The model's ability to produce sensible gap estimates over these out-of-estimation-sample episodes provides an informal assessment of the robustness of the original parameterization (see Section 3).

The Kalman smoother is conditioned on fourteen observable variables. The dataset includes standard national accounts aggregates—the growth rates of real per capita GDP, consumption, and investment—along with inflation measured by both the GDP deflator and core PCE inflation to extract a common signal of underlying price pressures. We include two measures of wage growth—compensation per hour and average hourly earnings—to similarly identify a latent wage inflation process robust to measurement error in individual series. Financial conditions are captured through the the federal funds rate and the corporate credit spread, defined as the difference between the Baa corporate rate and the 10-year Treasury yield. The labor market block is informed by four key variables: the unemployment rate, the LFPR, average hours worked per week (workweek), and vacancies. For the vacancy and workweek hours series, we apply an HP filter with smoothing parameter $\lambda = 10^5$ prior to feeding them into the smoother. This choice reflects the pronounced low-frequency trends observed in these variables over our sample period; the model does not include sufficiently persistent shocks to capture these very slow-moving movements, and the HP filter provides a more appropriate measure of the cyclical fluctuations the model is designed to explain. The model includes highly persistent shocks to labor supply preferences along the extensive margin, which allow it to capture the medium-frequency trends in participation directly.

The two ELB episodes in our sample—2008–2015 following the Global Financial Crisis and 2020–2021 during the pandemic—require special treatment because the zero lower bound constraint on nominal interest rates generates nonlinear dynamics that cannot be captured by standard linear solution methods. Following Kulish et al. (2017), we employ a piecewise-linear solution approach that approximates the economy's behavior during ELB periods by conditioning on the expected duration of the constraint at each point in time. We calibrate these expected durations using survey evidence: for the 2008–2015 episode, we rely primarily on the Blue Chip Economic Indicators survey and the Federal Reserve Bank of New York's Survey of Primary Dealers. For the 2020–2021 episode, we use the Survey of Primary Dealers throughout. The detailed construction of the expected ELB duration series is provided in Appendix A.5.

3 Model Validation

This section validates that our model generates realistic business cycle properties and sensible co-movements among key macroeconomic variables. The validation of this section serves two purposes. First, it establishes that the model's labor market mechanisms—search and matching frictions, endogenous participation and hours, and the interaction with nominal rigidities—operate sensibly when confronted with actual data. Second, it evaluates whether our calibration choices—setting steady-state values to longer-run assessments rather than sample averages, and incorporating time-varying monetary policy parameters from 2013 onward—materially compromise the model's structural properties or its ability to replicate business cycle patterns. We examine three dimensions of fit: unconditional business cycle volatilities, cyclical comovement with output, and the model-implied resource utilization gaps compared to external estimates from the Congressional Budget Office and Federal Reserve staff. Readers primarily interested in the construction and properties of the Structural Labor Market Indicator may proceed directly to Section 4, where we detail the indicator's methodology and historical behavior.

3.1 Unconditional Business Cycle Properties

Panel A of Table 2 reports standard deviations of key variables in the data and model, and Panel B reports their first-order autocorrelations.

Several patterns merit attention. The baseline model does a good job matching the volatility observed in the data across most variables. GDP volatility is reasonably captured (1.54 vs. 1.96), and labor market variables—unemployment, participation, vacancies, and workweek are close to their empirical counterparts, though the model displays somewhat smaller volatility than observed. The exceptions are consumption and investment, where the model understates volatility. Importantly, while labor market variables show slightly lower absolute volatility in the model, their volatility relative to output aligns well with the data, indicating that the model correctly captures the relative amplitudes of labor market fluctuations over the business cycle. Inflation volatility matches closely (0.12 vs. 0.14), and the nominal interest rate volatility is the same as in the data (0.37). In terms of autocorrelations, the model successfully matches the persistence observed in the data. GDP, unemployment, vacancies, and investment all display autocorrelations extremely similar to their empirical values, indicating that the model replicates not only

Table 2: Business Cycle Statistics: Data vs. Model

	GDP	u	LFPR	v	ww	w	π	i	c	I	spread
Panel A: Standard deviation (x100)											
Data	2.0	20.3	0.6	17.9	0.6	1.6	0.1	0.4	1.4	8.0	22.9
Model											
Baseline	1.5	16.7	0.5	15.6	0.6	0.7	0.1	0.4	0.8	3.0	34.2
Median	2.0	25.0	0.6	23.9	0.7	1.0	0.1	0.3	0.9	3.6	38.2
Min	1.7	19.5	0.5	18.6	0.6	0.8	0.1	0.2	0.8	3.2	36.7
Max	3.1	49.3	0.9	40.5	1.1	1.5	0.2	0.3	1.4	4.8	41.1
Panel B: Autocorrelation											
Data	0.96	0.98	0.92	0.96	0.90	0.93	0.42	0.96	0.95	0.98	0.87
Model											
Baseline	0.94	0.94	0.89	0.92	0.88	0.81	0.63	0.94	0.96	0.96	0.77
Median	0.93	0.94	0.89	0.92	0.87	0.78	0.67	0.97	0.95	0.96	0.75
Min	0.93	0.93	0.88	0.92	0.86	0.77	0.61	0.96	0.94	0.95	0.72
Max	0.93	0.95	0.91	0.93	0.89	0.80	0.77	0.98	0.95	0.96	0.76

Notes: All variables except interest rates and spreads are logged and HP-filtered with $\lambda = 10^5$. Each simulation generates a time series of length equal to the sample period (1987Q1–2025Q4), logs and HP-filters all variables identically to the data, and computes moments over 1,000 simulations. "Baseline" reports average statistics cross simulations and uses the constant pre-2013 Taylor rule coefficients throughout the sample. "Median," "Min,"and "Max" report the median, minimum, and maximum statistics, respectively, across simulations where the model uses the time-varying Taylor rule coefficients estimated for each historical period. Standard deviations are multiplied by 100 for easy reading. u: unemployment rate, LFPR: labor force participation rate, v: vacancies, ww: workweek, w: real wage, π: inflation, i: nominal interest rate, c: consumption, I: investment.

the volatility but also the persistence of business cycle fluctuations.

The median, minimum, and maximum statistics across the simulations using time-varying Taylor rule coefficients reveal that changes in the monetary policy rule do affect model-generated volatilities. The median volatilities tend to be higher than the baseline specification and, in some cases, exceed the data by a modest factor. However, these differences remain relatively contained, and the range between minimum and maximum values indicates that volatility does not change dramatically across different policy rule specifications. Similarly, the persistence properties of the model remain remarkably stable across specifications. This stability suggests that while the Taylor rule parameters influence the magnitude of business cycle fluctuations, they do not fundamentally alter the dynamic propagation mechanisms or the cyclical co-movement patterns that are central to the model's labor market structure.

3.2 Cross-Correlations and Dynamic Co-Movement

Figure 1 plots the cross-correlation functions between output and other key variables at leads and lags of up to eight quarters. The model does a good job matching the cross-correlation patterns observed in the data across both macroeconomic aggregates and labor market variables. For labor market variables, unemployment exhibits the expected strong negative contemporaneous correlation with output, with correlations remaining highly negative at both leads and lags, capturing the countercyclical nature of unemployment. Vacancies display mild leading behavior, with correlations rising 1-2 quarters before

Figure 1: Cross-Correlations with Output: Data vs. Model

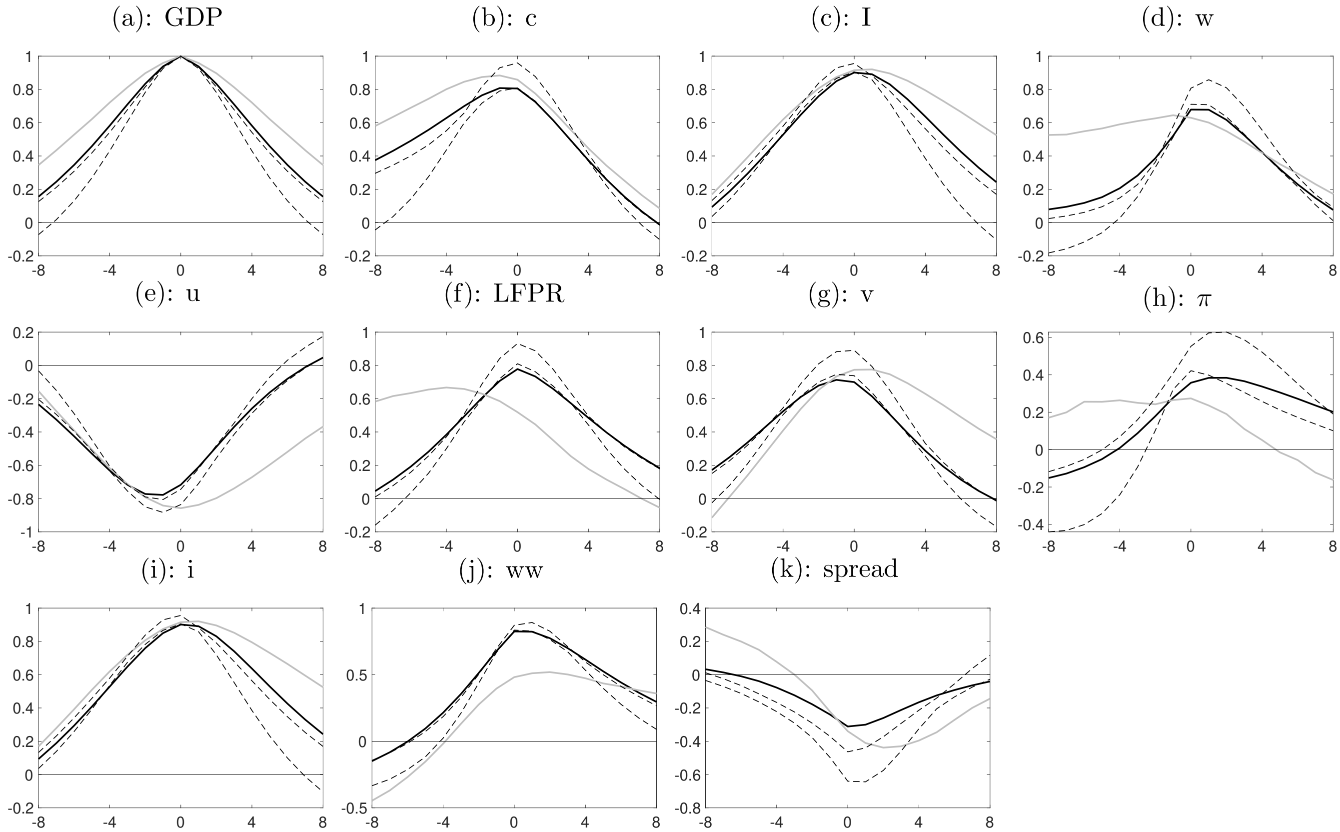

Notes: Cross-correlations computed from HP-filtered series ($\lambda = 10^5$). Solid gray lines: data; solid black lines: model average over 1,000 simulations using the baseline (constant pre-2013) Taylor rule. Dash-lines: minimum and maximum over the simulations that use a time-varying Taylor rule. Horizontal axis shows leads (positive) and lags (negative) in quarters. Each panel shows correlations between the indicated variable at time t and output at $t + j$.

output peaks. The labor force participation rate and workweek show positive contemporaneous correlations with output, indicating their procyclical nature, and these patterns are captured by the model. Wage growth displays positive correlation with output in both data and model, though the magnitude is somewhat understated in the model. Inflation shows weaker and more variable correlations with output, which the model also reproduces. Consumption shows strong contemporaneous correlation with output, and investment displays the characteristic leading behavior with peak correlations occurring slightly before output movements.

Importantly, simulations using time-varying Taylor rule coefficients generate similar cross-correlation functions to the baseline specification. While the monetary policy rule parameters affect the magnitude of business cycle volatility, as shown in Table 2, they do not alter the fundamental dynamic relationships between variables or their cyclical timing. This stability is particularly important for constructing a credible labor market indicator. The SLMI synthesizes information from multiple labor market variables to assess overall slack, and its reliability depends critically on the model correctly identifying how these variables relate to the business cycle. The fact that unemployment, vacancies, participation, hours, and wages all display appropriate lead-lag patterns and co-movement with output—and that these patterns

Figure 2: Model-Implied Gaps vs. External Estimates

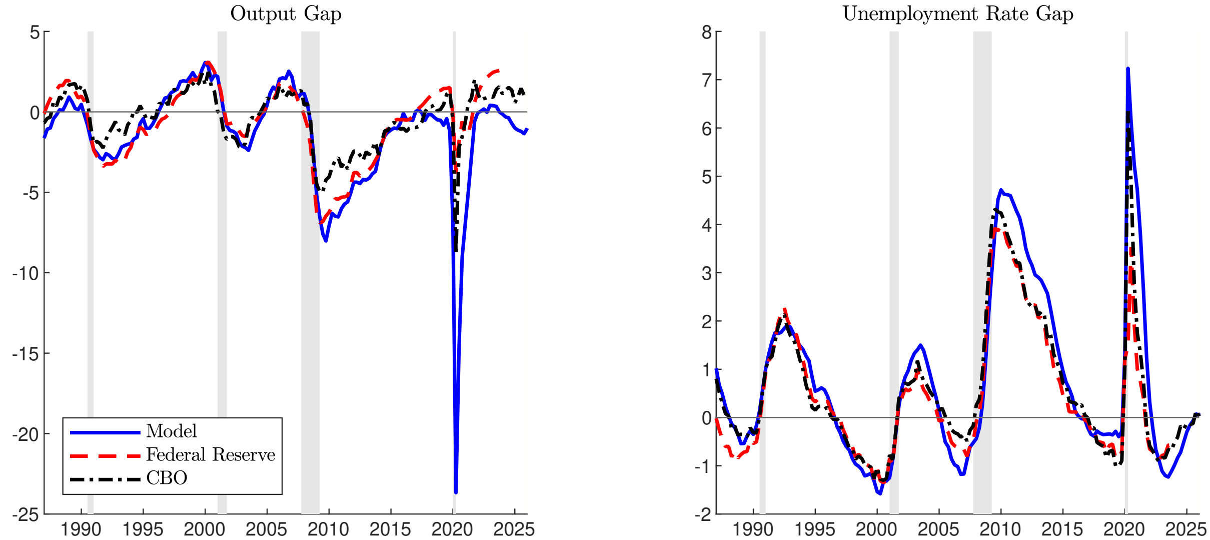

Notes: "Model" refers to our model's gaps, defined as deviations from flexible-price equilibrium, using the time-varying monetary policy rule. Federal Reserve estimates are based on the December 2020 Tealbook projections, which extend through 2023:Q4, and were retrieved via the Federal Reserve Bank of Philadelphia real-time database. CBO estimates are from the Congressional Budget Office. Shaded regions represent NBER recessions.

are robust to policy rule specification—provides confidence that the model captures the cyclical dynamics necessary to interpret labor market signals correctly.

3.3 External Validation: Resource Utilization Gaps

A more stringent test evaluates whether the model's estimates of unobservable slack align with independent assessments. Figure 2 compares the model-implied output gap and unemployment rate gap to estimates from the CBO and Federal Reserve Board staff.

Our model-based gaps are highly correlated with both CBO and Federal Reserve estimates, indicating substantial agreement on the cyclical position of the economy over the sample period. Despite this overall concordance, notable differences emerge in specific episodes. The model tends to identify greater slack during recessions than either the CBO or Federal Reserve estimates, a pattern that becomes more pronounced in the last two recessions. This is particularly evident during the COVID-19 recession, where our model's output gap shows a much larger decline than both the CBO and Federal Reserve assessments, reflecting the model's interpretation of the unprecedented collapse in economic activity and labor market outcomes. More recently, since 2024, the model indicates a small negative output gap, while CBO estimates show a positive gap. The unemployment rate gap comparisons show similar patterns. Despite these differences in specific episodes and the variation in gap magnitudes, the high correlation between our model-based gaps and these independent expert assessments gives us confidence that the model is capable of capturing the cyclical position of the labor market. The model's structural approach, which jointly interprets unemployment, participation, vacancies, hours, and wages through the lens of search and matching frictions and equilibrium conditions, provides a coherent framework for identifying labor market slack that aligns reasonably well with alternative methodologies that use different information sets and identifying assumptions.

Historically, the relationship between the output gap and the unemployment rate gap—the Okun's law—provides a natural benchmark for evaluating our model-based gaps. Using the CBO's estimates of potential output and the natural rate of unemployment, the Okun coefficient is approximately -1.0. The Federal Reserve's corresponding estimates yield a stronger relationship, with a coefficient of -1.68. Our model-based gaps produce an Okun coefficient of -1.7, which closely aligns with both the model's predicted unconditional relationship and the Federal Reserve's empirical estimate. This similarity validates that our flexible-price equilibrium concept generates unemployment-output co-movements consistent with standard measures of economic slack. Appendix C provides a visualization of the Okun's law relationship in our model over the sample period, as well as the the relationship using the gaps from the Federal Reserve and the CBO.

4 Constructing the SLMI: The Challenge of Multidimensional Labor Market Assessment

Policymakers routinely follow multiple labor market indicators that, at times, can send conflicting signals about the degree of labor market slack, complicating the assessment of appropriate policy. During 2015-2017, the unemployment rate hovered around 4.5 percent, suggesting relatively tight labor market conditions, yet the LFPR was declining, potentially indicating persistent slack as discouraged workers remained outside the labor force. In 2021-2022, unemployment remained low following the rapid pandemic recovery, but this co-existed with unusually low average workweek hours and exceptionally high vacancy rates, raising questions about whether standard unemployment metrics adequately captured labor market tightness. More recently, in 2025-2026, low unemployment has coincided with declining vacancies, presenting yet another configuration where different margins point in potentially different directions regarding labor market slack. Single indicators inevitably miss important information: the unemployment rate ignores the participation margin and the intensive margin of labor supply; the vacancy-to-unemployment ratio, while capturing labor demand relative to job seekers, abstracts from hours worked. These shortcomings motivate a central question of this paper: can we synthesize information across multiple labor market margins—unemployment, participation, vacancies, hours, and wages—to construct a comprehensive assessment of overall labor market slack? Our contribution is to use the structural model presented in Section 2 to extract a common signal about the state of the labor market from multiple indicators. By computing model-based gaps for each labor market variable—defined as deviations from their flexible-price equilibrium counterparts—and identifying the common factor underlying their joint variation, we construct a Structural Labor Market Indicator (SLMI) that provides a unified, model-consistent measure of labor market slack that incorporates information from all observable margins simultaneously.

Figure 3: Model-Based Labor Market Gaps and SLMI

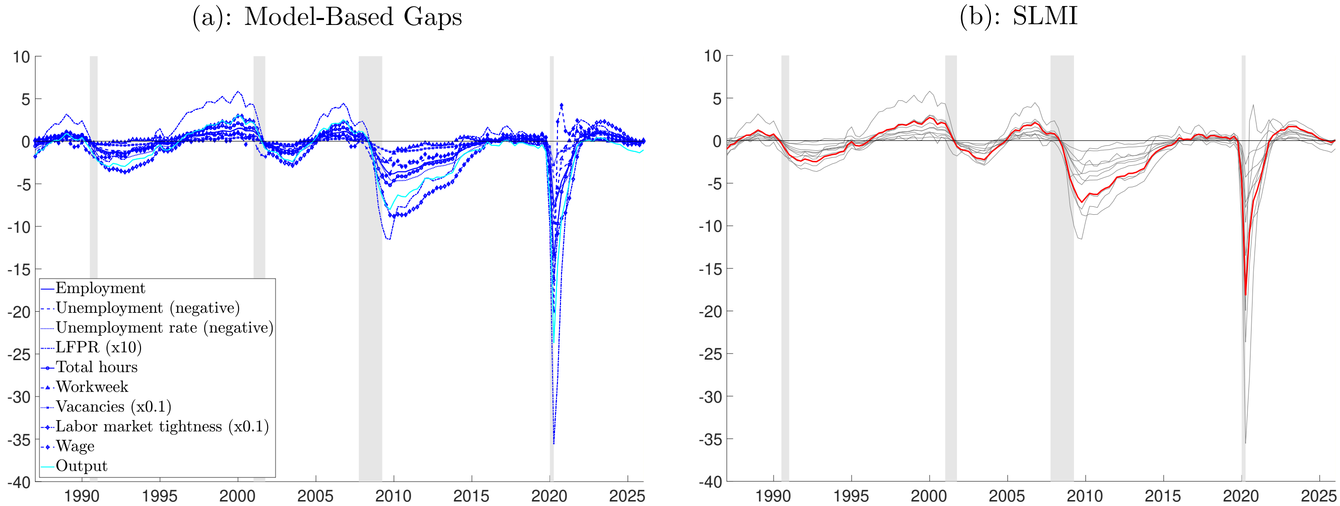

Notes: Red and gray lines in panel 3(b) represent the SLMI and all model-based gaps presented in panel 3(a), respectively. Shaded regions represent NBER recessions.

4.1 Individual Variable Signals

We define labor market gaps as deviations of observed variables from their flexible-price-and-wage equilibrium values. This counterfactual equilibrium represents the state of the labor market in the absence of nominal price and wage rigidities and exogenous markup shocks. Thus, our gaps measure is fundamentally a model-based concept. Importantly, this flexible equilibrium is not the efficient allocation: it retains all real frictions present in the economy. The gaps therefore capture cyclical deviations from an equilibrium that reflects the economy's structural features—the natural rates of unemployment, participation, and output—rather than deviations from a first-best optimum.

Figure 3(a) presents our model-based labor market gaps for nine key labor market variables: the level of employment, the level of unemployment, the unemployment rate, the labor force participation rate, vacancies, total hours worked, average workweek hours, labor market tightness as defined in the model (i.e., ratio of vacancies to job searchers), and real wages. Some gaps are scaled to facilitate visual comparison across variables with different units and volatilities.[2] Not surprisingly, the gaps are highly correlated over the full sample period, reflecting the common cyclical forces that drive labor market fluctuations—all gaps move together during major recessions and expansions, indicating broadly coherent signals about labor market slack during these episodes. However, examining specific time windows reveals important divergences that motivate the need for a synthetic indicator, especially at turning points as highlighted before.

[2]Figure A.3 in Appendix B plots each gap separately.

Table 3: Weights in SLMI

E	U	u	LFPR	H	ww	v	θ	w
0.23	-0.32	-0.20	0.67	0.17	0.27	0.07	0.01	0.12

Notes: This table presents the weights on the model-based labor market gaps used in the construction of the structural labor market indicator. E: employment, U: unemployment, u: unemployment rate, LFPR: labor force participation rate, H: total hours, ww: workweek, v: vacancies, θ: labor market tightness, w: real wage.

4.2 Aggregation into SLMI

To synthesize the information contained in these multiple labor market gaps into a single summary measure, we employ principal component analysis (PCA).[3] The application of PCA to our nine labor market gaps reveals a strong common factor structure. As we show below, the first principal component alone accounts for the vast majority of the total variance across all gaps and is the only component with an eigenvalue exceeding one—indicating that it explains more variance than any single original variable. This finding validates our approach: the dominant first principal component captures the shared cyclical information across all labor market indicators, providing a natural one-dimensional summary of overall labor market slack. Based on this first principal component, we define our Structural Labor Market Indicator (SLMI). By construction, the SLMI represents the optimal linear combination of the individual gaps in terms of explaining their joint variation, providing a model-based, comprehensive measure of labor market slack or tightness.

The construction of the SLMI proceeds in three steps. First, we normalize all labor market gaps by subtracting their respective sample means and dividing by their respective sample standard deviations. This standardization ensures that each variable contributes to the principal component analysis on an equal footing, preventing variables with larger variances from dominating the extracted factor. Second, we apply PCA to the standardized gaps and extract the loadings (weights) associated with the first principal component. Third, we construct the SLMI as a weighted average of the original (non-standardized) gaps, where the weights are the first principal component loadings normalized by each gap's sample standard deviation. This final step ensures that the SLMI retains the level information present in the original gaps: unlike a standard principal component computed from standardized data, our SLMI has a non-zero mean that reflects the average state of labor market slack over the sample period. This property is crucial for interpretation—it means that an SLMI value of zero corresponds to neutral labor market slack. Consequently, the indicator avoids the potential bias where zero would mechanically represent balanced conditions even when all underlying gaps systematically indicate labor market slack or tightness.

Table 3 presents the weights for each labor market gaps used in the construction of the SLMI, and the red line in Figure 3(b) presents the SLMI. Not surprisingly, the SLMI lies within the range spanned by the

[3] PCA is a statistical technique that extracts common signals from multivariate data without requiring a pre-specified model or prior knowledge of the underlying system dynamics. Its primary strength lies in dimensionality reduction: it identifies orthogonal components that capture the maximum variance in the data, effectively filtering out idiosyncratic noise while preserving systematic co-movements. Unlike traditional filtering methods that impose strict assumptions about the data-generating process, PCA is purely data-driven, making it particularly robust for discovering latent patterns that drive multiple economic variables simultaneously. This approach is especially well-suited to our context, where labor market gaps are expected to share a common cyclical component but may also exhibit indicator-specific dynamics.

Figure 4: Historical Decomposition SLMI

(a): Shock Decomposition (b): Data Decomposition

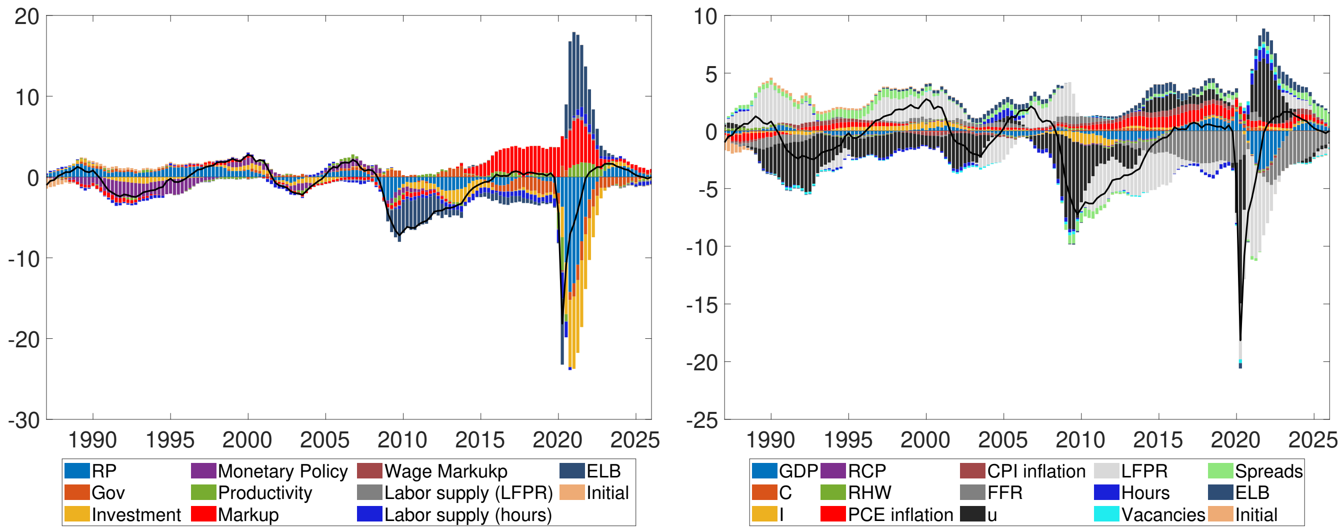

Notes: Panel 4(a) presents the historical shock decomposition of the SLMI, showing the contribution of each structural shock to the deviation of the SLMI from its steady state over the sample period. Panel 4(b) presents the data decomposition, indicating the contribution of each observable variable used in the model's estimation to the SLMI dynamics. Both decompositions sum to the total SLMI value shown by the solid black line.

individual indicators, reflecting its role as a weighted average of these gaps. During periods when all labor market indicators move decisively in the same direction—such as the deep recessions of the early 1980s, 2008-2009, and 2020—the SLMI provides an unambiguous signal of substantial labor market slack or tightness. However, at turning points in the business cycle, when the economy transitions from expansion to recession or from recession to recovery, the individual gaps often provide conflicting assessments of labor market slack. It is precisely in these episodes that the SLMI proves most valuable, synthesizing the divergent signals into a single coherent measure of overall labor market slack. In Section 5, we examine more closely how the SLMI and the unemployment rate—often considered the primary indicator of labor market slack—have provided different signals at critical historical junctures. Similarly, Section 5 also shows that the SLMI outperforms taking the principal component of the detrended data in multiple dimensions. Before that, we show next the historical decomposition of the SLMI, its drivers and sources of information.

4.3 Historical Evolution of the SLMI: Shock and Data Decompositions

Figure 4 presents two complementary perspectives on the SLMI's evolution over time. Figure 4(a) displays the shock decomposition, showing how different structural disturbances have contributed to the SLMI at each point in the sample. Figure 4(b) presents the data decomposition, illustrating which observable variables have been most informative in shaping the SLMI's movements.[4]

The shock decomposition reveals that the primary drivers of labor market slack over our sample

[4]Figure A.5 in Appendix D presents the double decomposition, which attributes SLMI variation simultaneously to specific shocks and specific observables following the methodology in Chung et al. (2021).

period have been risk premium shocks—which operate as aggregate demand disturbances—and investment efficiency shocks—which function as supply-side disturbances. These two shock categories account for the bulk of SLMI variation, with risk premium shocks predominantly driving the deep labor market slack during the 2008-2009 financial crisis and the COVID-19 recession, while investment efficiency shocks contributed importantly to both the 2001 downturn and the slow recovery following the Great Recession. Markup shocks and productivity shocks play more modest roles, contributing to shorter-run fluctuations but rarely dominating the SLMI's movements. It is particularly worth noting the time-varying importance of monetary policy shocks. Before 2013, when our model employs a constant Taylor rule, monetary policy shocks explain a non-trivial portion of SLMI variation, particularly during the early 1990s and early 2000s. However, since 2013, when we incorporate time-varying Taylor rule coefficients that better capture the FOMC's evolving systematic responses to economic conditions, monetary policy shocks become negligible contributors to the SLMI. This shift suggests that the time-varying rule captures well the behavior of monetary policy over this period.

The data decomposition provides complementary insights into which observable variables have been most informative about labor market slack. Unsurprisingly, the unemployment rate and the LFPR emerge as the consistently most informative variables throughout the sample, reflecting that these series directly measure labor market quantities and are observed with relatively little measurement error. However, the decomposition also reveals that all other variables, in various combinations, have contributed meaningfully to the SLMI in different periods, underscoring the value of the multi-variable approach. In recent years, GDP growth has proven particularly informative about the SLMI's assessment of labor market slack. Between 2020 and 2021, GDP growth indicated persistent slack in the labor market despite the rapid recovery in the unemployment rate. Since 2024, GDP growth has suggested modestly tight labor market conditions despite an unemployment rate slightly above its estimated natural rate. This pattern highlights one of the key benefits of our model-based indicator: looking at labor market data in isolation does not provide a complete picture of labor market slack. The structural model synthesizes information from both labor market and non-labor market variables through equilibrium conditions that link labor demand to aggregate activity. Intuitively, if GDP is growing strongly with low inflation, and a relatively stable unemployment rate that is not unusually low, this configuration suggests slack in the labor market—the economy is expanding without generating wage-price pressures, indicating unutilized labor resources. Conversely, the same unemployment rate could imply tight labor market conditions if it coincides with high inflation and only moderate GDP growth, as this pattern suggests supply constraints binding labor utilization. The SLMI captures these context-dependent interpretations by filtering all observable information through the model's structural relationships.

To further analyze the informational content of non-labor market data, we implement a two-stage decomposition illustrated in Figure 5. Figure 5(a) compares two versions of the SLMI: one constructed using the full dataset (solid black line) and another using only labor market observables (red line). The gap between the two indicators quantifies the informational role played by non-labor market data in shaping our slack assessment. During the pandemic recovery (2020–2021), the labor-market-only SLMI

Figure 5: The Role of Non-Labor Market Data

(a): SLMI: Full Data vs. Labor Market Data Only

(b): Data Decomposition: Non-Labor Data

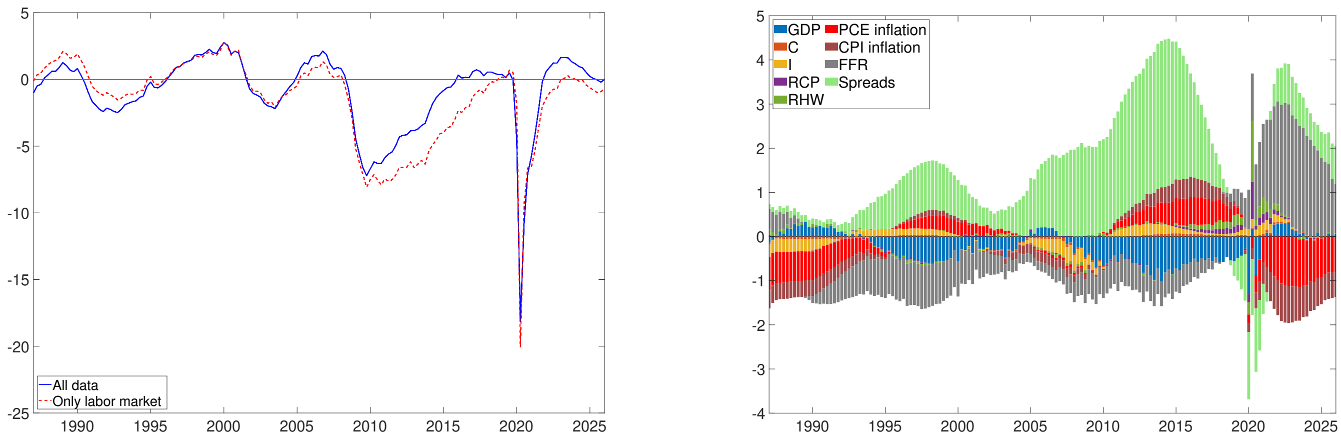

Notes: Panel 5(a) presents the SLMI constructed using all available data (solid black line) and using only labor market variables (solid red line). Panel 5(b) presents the data decomposition of non-labor market variables to the gap between the two indicators in Panel 5(a).

suggests noticeably less slack than the full-information indicator, failing to capture the persistent resource underutilization signaled by weak GDP growth despite rapid unemployment recovery. In recent years (2024-2026), the labor-only indicator points to tighter conditions than the full SLMI.

Figure 5(b) decomposes the gap between the full dataset and the labor-market-only SLMI into contributions from non-labor market variables. GDP growth (blue) and inflation emerge as important contributors. In 2020-2021, when unemployment had already declined sharply, GDP growth signals persistent slack and, in 2021-2023, inflation (PCE in red and CPI in maroon) validate tightness even as some labor margins were ambiguous. Credit spreads and the federal funds rate also play non-negligible roles. Credit spreads (light green) contribute substantially to the SLMI gap especially in periods of financial stress. For example, credit spreads make a positive contribution to the SLMI during the 2008-2009 financial crisis, suggesting that the labor market was tighter than labor market variables would indicate. In contrast, during the COVID-19 recession, spreads contribute negatively, reinforcing the slack signal. The federal funds rate (gray) also makes sizable contributions thoroughout the sample. Finally, non-labor market data account for almost 19% of the SLMI variance over the sample period.[5] Therefore, we conclude that a comprehensive assessment of labor market slack requires looking beyond labor market aggregates.

5 Comparing the SLMI to Alternative Measures: Is the Unemployment Rate a Sufficient Statistic?

Figure 6 presents our model-based SLMI (solid black line) alongside alternative measures of aggregate labor market slack that are model-free and thus purely empirical. Figure 6 includes the Kansas City

[5] The covariance between the labor-market and non-labor-market contributions is negative indicating that those two types of data often provide offsetting signals about slack, which reinforces the value of incorporating both types of information as they provide complementary rather than redundant assessments of labor market conditions.

Figure 6: SLMI and Alternative Labor Market Gaps

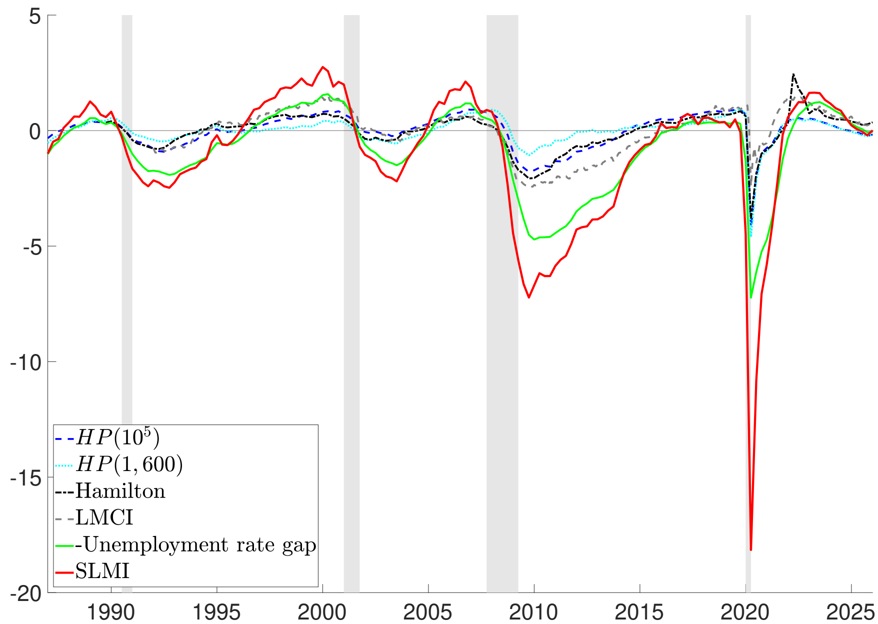

Notes: $HP(10^5)$: first principal component of the labor market data when filtered with the HP filter and a smoothing parameter equal to 10^5. $HP(1,600)$: first principal component of the labor market data when filtered with the HP filter and a smoothing parameter equal to $1,600$. Shaded regions represent NBER recessions.

Fed Labor Market Condition Indicator (LMCI), which is a data-based indicator based on labor-market data only (Hakkio and Willis, 2014). Figure 6 also includes three variants of a principal component analysis applied directly to the filtered labor-market data: the first principal component extracted from our six labor market variables after applying an HP filter with smoothing parameter $\lambda = 10^5$ (dashed line), the same exercise with $\lambda = 1,600$ (dotted line), and the first principal component after applying the Hamilton filter (dash-dotted line). For comparison, we also plot our model-based unemployment rate gap (gray line), which represents the deviation of the unemployment rate from its flexible-price-and-wage equilibrium counterpart.

Several noteworthy patterns emerge from this comparison. First, the SLMI tends to provide earlier warning signals of deteriorating labor market conditions: it typically turns negative before the alternative indicators at recession onset, most notably prior to the 2001 and 2008 recessions. However, the SLMI also exhibits slower recovery dynamics, lagging behind the filtered-data measures during the expansion phases of the mid-1990s and 2010s. This asymmetry reflects the model's richer propagation mechanisms, where labor market slack dissipates more gradually through the interaction of search frictions, participation decisions, and hours adjustments. Second, in contrast to our model-based gaps where the first principal component explains the vast majority of the variance and is the only component with an eigenvalue exceeding one, the purely data-driven principal component analysis exhibits a less concentrated factor structure. When applied to filtered data, up to three principal components explain more than two variables' worth of volatility, suggesting that the common cyclical signal is more diffuse without the discipline imposed by the structural model. Third, while the SLMI and the unemployment rate gap are highly correlated over the full sample, they occasionally provide divergent signals about labor market slack.

A prominent example occurs in 2021, when the SLMI indicated emerging labor market tightness earlier than the unemployment rate gap, capturing dimensions of labor market pressure beyond unemployment dynamics alone.

The advantages of our model-based approach become clear in this comparison. Relative to purely statistical measures constructed from filtered data, our theoretical framework allows us to conduct counterfactual analysis, decompose the indicator into contributions from specific economic shocks, and perform sensitivity analysis with respect to assumptions about longer-run trends and natural rates—exercises that are not feasible with atheoretical filtering methods. Furthermore, the model's explicit treatment of multiple labor market margins means the SLMI naturally aggregates information from unemployment, labor force participation, vacancies, and hours worked in a way that respects their structural relationships. The high correlation between our unemployment rate gap and the SLMI is unsurprising but revealing: both measures are constructed using the discipline of a structural model estimated on a rich dataset that encompasses not only multiple labor market variables but also spending data and inflation dynamics. *This means that our model-based unemployment gap itself already incorporates information from the broader macroeconomic environment*—it is not simply a filtered unemployment series but rather an equilibrium outcome informed by all the data used to discipline the model. The SLMI takes this a step further by aggregating the model-implied gaps across multiple labor market dimensions, each of which has been inferred using this comprehensive information set. Compared to relying solely on the unemployment rate gap, the SLMI's incorporation of these additional dimensions proves particularly valuable during episodes when labor market slack manifests along other margins of labor adjustment. The 2021-2022 period exemplifies this advantage: while the unemployment rate remained above pre-pandemic levels, the SLMI detected tightening conditions by incorporating signals from surging vacancies and rising hours worked. This multi-dimensional perspective provides policymakers with a more complete assessment of labor market resource utilization than any single indicator can deliver.

6 Uncertainty and the One-Sided Filter

While the SLMI provides a comprehensive summary of labor market slack, policymakers naturally care about the precision of such estimates. Any model-based indicator is subject to various sources of uncertainty, including parameter uncertainty, shock identification, and specification choices. Moreover, policymakers require indicators that can be computed in real time, without the benefit of revised data or future observations. We address both concerns by constructing credible intervals for the SLMI that quantify parameter uncertainty and by comparing the smoothed SLMI to its real-time counterpart.

6.1 Credible Intervals

We construct credible intervals for the SLMI using Monte Carlo simulations that account for parameter uncertainty. Specifically, we assume that our model parameters follow a multivariate normal distribution centered at our baseline calibrated values, with variance-covariance matrix Σ. To construct Σ, we

Figure 7: SLMI 68% Credible Intervals

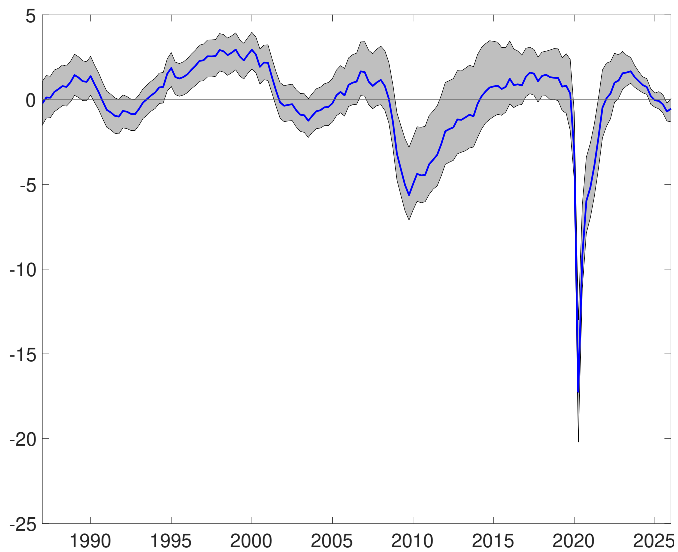

Notes: Shaded region represents the 68 percent credible interval. The blue line corresponds to the median SLMI.

partition the full parameter vector into three blocks and assume zero covariance across blocks: (i) the time-varying monetary policy rule coefficients, (ii) the calibrated parameters reported in Table 1, and (iii) the parameters adopted from Cairó et al. (2026). This block-diagonal structure reflects our sequential calibration strategy and the different data sources used to discipline each parameter subset. For the time-varying Taylor rule parameters, we compute the variance-covariance matrix using the 4,000 posterior draws from González-Astudillo and Tanvir (2026). For the parameters taken from Cairó et al. (2026), we similarly compute the variance-covariance matrix directly from their posterior draws. For the calibrated parameters in Table 1, we proceed as follows. We use the time series of median SEP for the longer-run values of the federal funds rate, unemployment rate, and GDP growth to compute the variance-covariance matrix across these longer-run targets, which discipline our steady-state calibration. For the markup shock persistence parameter ρ^{ϵ_p}, we assume an independent normal distribution with standard deviation of 0.1, and zero correlation with other parameters. Drawing $100,000$ parameter vectors from this multivariate normal distribution, we re-solve the model and re-compute the SLMI for each draw, generating the 68 percent credible intervals presented in Figure 7.

Figure 7 reveals several notable features of the uncertainty surrounding the SLMI. The credible intervals exhibit a modest downward skew, indicating that the distribution of possible SLMI values tends to be asymmetric with a slightly heavier tail toward greater labor market tightness. In recent years, the credible intervals have narrowed considerably, reflecting increased confidence in the estimated values of labor market slack and suggesting that parameter uncertainty has less impact on the SLMI during this period. A particularly instructive episode is the recovery from the Great Recession: during much of the 2010-2015 period, the credible intervals include zero, indicating substantial model uncertainty about the timing and pace of labor market normalization. This uncertainty captures genuine ambiguity about whether labor markets had returned to equilibrium conditions during this prolonged recovery phase, a period when policymakers and economists actively debated the degree of remaining labor market slack.

6.2 One-Sided Filter

For practical policy applications, an important consideration is whether the SLMI can be computed using only information available to policymakers at each point in time. The SLMI presented throughout this paper is constructed using the Kalman smoother, which is a two-sided filter that conditions on the full sample of data—past, present, and future observations. While this approach yields the most accurate estimates of historical labor market conditions, it is not directly implementable in real time. We therefore construct a version of the SLMI using the one-sided Kalman filter, which conditions only on information available up to time t when estimating the state of the economy at time t.

Figure 8: SLMI: Two-Sided vs. One-Sided Filters

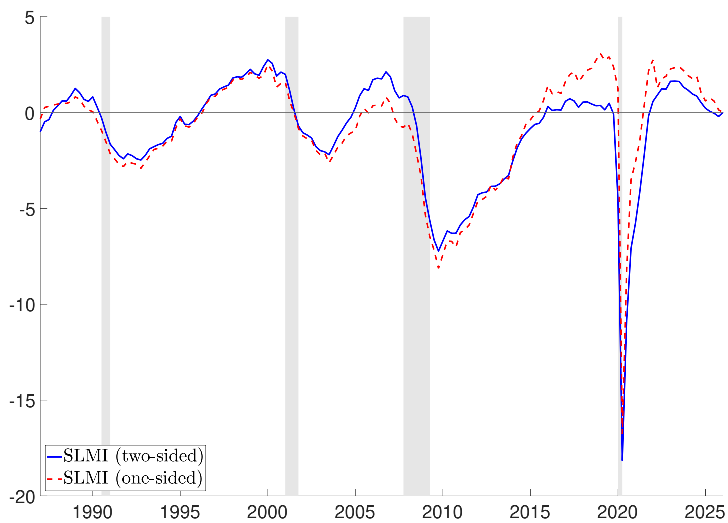

Notes: Shaded regions represent NBER recessions.

Figure 8 compares the smoothed (two-sided) SLMI to its one-sided filter counterpart over the sample period. The two series are highly correlated, confirming that the SLMI provides reliable signals even when computed in real time without the benefit of future data revisions. However, a systematic difference emerges: the one-sided indicator has been visibly higher on average since 2015, suggesting that it tends to overestimate labor market tightness to some extent. Despite this tendency, the one-sided SLMI preserves the key property established earlier in the paper: it continues to provide earlier warning signals of deteriorating labor market conditions relative to alternative indicators. This combination of timeliness and implementability makes the real-time SLMI a practical tool for policymakers who must assess labor market conditions without the luxury of hindsight.

7 Conclusion

Assessing labor market slack is most difficult precisely when it matters most: at business cycle turning points, when participation, hours, vacancies, and wages may send conflicting signals about resource utilization. The unemployment rate, though informative, is silent on these other margins, while purely statistical aggregators of labor market data cannot separate supply from demand, draw on non-labor information or support counterfactual analysis. This paper develops a Structural Labor Market Slack (SLMI) indicator that addresses these shortcomings, synthesizing information across nine labor market dimensions using a medium-scale DSGE model with search and matching frictions, endogenous participation, and variable hours. By defining slack relative to a flexible-price-and-wage equilibrium and disciplining the model on a comprehensive dataset spanning both labor market and macroeconomic variables, we obtain a theoretically coherent, empirically validated measure of overall slack for the U.S. economy over 1987–2026.

Our analysis yields four main findings with policy relevance. First, the SLMI frequently diverges from alternative measures at critical junctures, tending to warn earlier of deterioration at recession onset while recovering more gradually during expansions, an asymmetry that reflects the model's richer propagation through search frictions, participation, and hours. Second, and crucially, data decompositions show that GDP growth and inflation carry substantial information about labor market slack beyond what labor market variables alone reveal. The same unemployment rate can signal different degrees of slack depending on whether it coincides with strong growth and subdued inflation or weak growth and elevated price pressures. Third, shock decompositions attribute the bulk of labor market fluctuations to aggregate demand disturbances (risk premium shocks) and supply-side factors (investment efficienct shocks), while monetary policy shocks play a negligible role once we allow for time-varying systematic policy responses. Fourth, the indicator is practical for real-time use and admits formal uncertainty quantification: the one-sided, real-time SLMI tracks its smoothed counterpart closely and preserves the early-warning property, and Monte-Carlo credible intervals reveal that parameter uncertainty is especially elevated during recoveries. During much of the 2010–2015, for example, the 68 percent intervals straddle zero, capturing the genuine ambiguity policymakers faced over the pace of normalization.

Important limitations qualify our results and suggest directions for future research. The SLMI is inherently model-dependent, requiring judgment about structural features, calibration of long-run natural rates, and shock specifications. The reliance on time-varying monetary policy rule coefficients estimated from Summary of Economic Projections data limits this feature to the post-2013 period, and alternative specifications of the policy rule could affect the attribution of movements to systematic policy versus shocks. Future work could extend the analysis by incorporating additional labor market heterogeneity such as skill mismatch or industry-specific dynamics, exploring alternative equilibrium concepts for defining slack. Nevertheless, our structural approach demonstrates that meaningful progress can be made in constructing comprehensive labor market slack measures that respect theoretical coherence while maintaining strong empirical performance, providing policymakers with a valuable tool for navigating the inherently multidimensional challenge of assessing labor market slack.

References

Bauer, Michael D, Carolin E Pflueger, and Adi Sunderam, "Perceptions About Monetary Policy," *The Quarterly Journal of Economics*, 11 2024, *139* (4), 2227–2278.

Bernanke, Ben S., Mark Gertler, and Simon Gilchrist, "The Financial Accelerator in a Quantitative Business Cycle Framework," in J. Taylor and M. Woodford, eds., *J. Taylor and M. Woodford, eds.*, Vol. 1 of *Handbook of Macroeconomics*, Elsevier, 1999, pp. 1341–1393.

Blagrave, Patrick, Roberto Garcia-Saltos, Douglas Laxton, and Fan Zhang, "A Simple Multivariate Filter for Estimating Potential Output," 2015.

Boivin, Jean, "Has U.S. Monetary Policy Changed? Evidence from Drifting Coefficients and Real-Time Data," *Journal of Money, Credit and Banking*, 2006, *38* (5), 1149–1173.

_ **and Marc P. Giannoni**, "Has Monetary Policy Become More Effective?," *The Review of Economics and Statistics*, 2006, *88* (3), 445–462.

Cacciatore, Matteo, Giuseppe Fiori, and Nora Traum, "Hours and Employment over the Business Cycle: A Structural Analysis," *Review of Economic Dynamics*, 2020, *35*, 240–62.

Cairó, Isabel, Hess T. Chung, Francesco Ferrante, Cristina Fuentes-Albero, Camilo Morales-Jiménez, and Damjan Pfajfar, "Endogenous Labor Supply in an Estimated New-Keynesian Model: Nominal versus Real Rigidities," Technical Report May 2026.

_ **, Shigeru Fujita, and Camilo Morales-Jiménez**, "The Cyclicality of Labor Force Participation Flows: The Role of Labor Supply Elasticities and Wage Rigidity," *Review of Economic Dynamics*, January 2022, *43*, 197–216.

Campolmi, Alessia and Stefano Gnocchi, "Labor Market Participation, Unemployment and Monetary Policy," *Journal of Monetary Economics*, 2016, *79*, 17–29.

Christiano, Lawrence J, Martin S Eichenbaum, and Mathias Trabandt, "Understanding the Great Recession," *American Economic Journal: Macroeconomics*, 2015, *7* (1), 110–167.

Christiano, Lawrence J., Mathias Trabandt, and Karl Walentin, "Involuntary Unemployment and the Business Cycle," *Review of Economic Dynamics*, 2021, *39* (1), 26–54.

Chung, Hess, Bruce Fallick, Christopher J. Nekarda, and David Ratner, "Assessing the Change in Labor Market Conditions," *FEDS Notes. Washington: Board of Governors of the Federal Reserve System*, 2014, *May 22*, 35–49.

_ **, Cristina Fuentes-Albero, Matthias Paustian, and Damjan Pfajfar**, "Latent variables analysis in structural models: A New decomposition of the kalman smoother," *Journal of Economic Dynamics and Control*, 2021, *125*, 104097.

Clarida, Richard, Jordi Galí, and Mark Gertler, "Monetary Policy Rules and Macroeconomic Stability: Evidence and Some Theory," *The Quarterly Journal of Economics*, 2000, *115* (1), 147–180.

Congressional Budget Office, "The Budget and Economic Outlook: 2026 to 2036," 2026.

Elsby, Michael W.L., Bart Hobijn, and Ayşegül Şahin, "On the importance of the participation margin for labor market fluctuations," *Journal of Monetary Economics*, 2015, *72*, 64–82.

González-Astudillo, Manuel and Rakeen Tanvir, "Hawkish or Dovish? Inferring intended monetary policy from the Fedâs dot plot," *Journal of Economic Dynamics and Control*, 2026, *185*, 105294.

Gordon, Robert J., "The Time-Varying NAIRU and Its Implications for Economic Policy," *Journal of Economic Perspectives*, March 1997, *11* (1), 11â32.

Hakkio, Craig S. and Jonathan L. Willis, "Kansas City Fed's Labor Market Conditions Indicators (LMCI)," *Federal Reserve Bank of Kansas City, The Macro Bulletin*, 2014, *August 28.*

Holston, Kathryn, Thomas Laubach, and John C. Williams, "Measuring the natural rate of interest: International trends and determinants," *Journal of International Economics*, 2017, *108*, S59–S75. 39th Annual NBER International Seminar on Macroeconomics.

Jaimovich, Nir and Sergio Rebelo, "Can News about the Future Drive the Business Cycle?," *American Economic Review*, 2009, *99* (4), 1097–1118.

Kiley, Michael T., "Output gaps," *Journal of Macroeconomics*, 2013, *37*, 1–18.

Krusell, Per, Toshihiko Mukoyama, Richard Rogerson, and Ayşegül Şahin, "Gross Worker Flows Over the Business Cycle," *American Economic Review*, 2017, *107* (11), 3447–3476.

_ , _ , _ , and _ , "Gross Worker Flows and Fluctuations in the Aggregate Labor Market," *Review of Economic Dynamics*, 2020, *37* (1), s205–s226.

Kulish, Mariano, James Morley, and Tim Robinson, "Estimating DSGE models with zero interest rate policy," *Journal of Monetary Economics*, 2017, *88*, 35–49.

Laubach, Thomas and John C. Williams, "Measuring the Natural Rate of Interest," *The Review of Economics and Statistics*, 2003, *85* (4), 1063–1070.

Nucci, Francesco and Marianna Riggi, "Labor Force Participation, Wage Rigidities, and Inflation," *Journal of Macroeconomics*, 2018, *55*, 274–92.

Orphanides, Athanasios and John C. Williams, "Robust Monetary Policy Rules with Unknown Natural Rates," *Brookings Papers on Economic Activity*, 2002.

Primiceri, Giorgio E., "Time Varying Structural Vector Autoregressions and Monetary Policy," *The Review of Economic Studies*, 07 2005, *72* (3), 821–852.

Staiger, Douglas, James H. Stock, and Mark W. Watson, "The NAIRU, Unemployment and Monetary Policy," *Journal of Economic Perspectives*, March 1997, *11* (1), 33â49.

Supplemental Appendix

Beyond the Unemployment Rate: A Structural Labor Market Indicator

Isabel Cairó[3] Hess Chung[3] Francesco Ferrante[3] Cristina Fuentes-Albero[3] Camilo Morales-Jiménez[3] Damjan Pfajfar[4]

July 2026

A Model Details and Equations

A.1 Summary of Equations for the Rigid Economy

This section presents the equations for the rigid economy. In particular, there are 64 endogenous variables,

$$L_t, N_t, U_t, H_t, s_t, u_t, \tilde{\mathcal{U}}_t, \tilde{c}_t, \tilde{X}_t(l), \tilde{X}_t(h), zh_t, \tilde{L}_{ct}, \tilde{\nu}_t(l), \tilde{\nu}_t(h), \tilde{V}_{ct}, \tilde{V}_{ht}, \tilde{V}_{zht}, \tilde{w}_t, R_t, \tilde{\Lambda}_{t,t+1},$$

$$\tilde{b}_t, \tilde{\mu}_t, \tilde{V}^h_t, p_t, m_t, v_t, q_t, \theta_t, \pi_t, p^m_t, \tilde{mpl}_t, mpk_t, r^k_t, \tilde{\Omega}_t, \tilde{\epsilon}^{avg}_{t,t}, \tilde{\mu}^{avg}_{t,t}, \tilde{\chi}^{avg}_{t,t}, \tilde{\kappa}_{vt}, \tilde{\kappa}_{nt}, z_t, \tilde{J}_t, \tilde{w}^0_t, \delta_{kt},$$

$$a_t, u^k_t, R^k_t, q^k_t, \tilde{I}_t, \hat{z}_{\omega t}, \hat{G}_t, \hat{G}'_t, \bar{\omega}_t, \hat{\Gamma}_t, \hat{\Gamma}'_t, \phi_t, \tilde{N}_{wt}, \tilde{K}_t, i_t, hours\_gap_t, \tilde{Y}_t, spread_t, default_t, \tilde{k}_t, \widetilde{GDP}_t$$

and the following 64 equations:
Households:

$$N_t = (1-\delta_{st})N_{t-1} + p_t s_t \tag{A.1}$$

$$\tilde{X}_t(h) = (\tilde{c}_t - h\tilde{c}_{t-1}/\gamma_t)^{\gamma_h}\left(\tilde{X}_{t-1}(h)/\gamma_t\right)^{1-\gamma_h} \tag{A.2}$$

$$\tilde{X}_t(l) = (\tilde{c}_t - h\tilde{c}_{t-1}/\gamma_t)^{\gamma_l}\left(\tilde{X}_{t-1}(h)/\gamma_t\right)^{1-\gamma_l} \tag{A.3}$$

$$L_t = N_t + U_t \tag{A.4}$$

$$H_t = N_t + \Gamma U_t \tag{A.5}$$

$$L_t = s_t + (1-\delta_{st})N_{t-1} \tag{A.6}$$

$$u_t = \frac{U_t}{L_t} \tag{A.7}$$

$$\tilde{\mathcal{U}}_t = \tilde{c}_t - h\frac{\tilde{c}_{t-1}}{\gamma_t} + \chi_{lt}\frac{(1-H_t)^{(1-\alpha_h)(1-\psi_l)}}{1-\psi_l}\tilde{X}_t(l) - \chi_{ht}\frac{zh_t^{1+\psi_h}}{1+\psi_h}N_t\tilde{X}_t(h) \tag{A.8}$$

[‡]Board of Governors of the Federal Reserve System. *Email addresses*: isabel.cairo@frb.gov (I. Cairó), hess.t.chung@frb.gov (H. Chung), francesco.ferrante@frb.gov (F. Ferrante), cristina.fuentes-albero@frb.gov (C. Fuentes-Albero), camilo.moralesjimenez@frb.gov (C. Morales-Jiménez).

[§]*Address:* Federal Reserve Bank of Cleveland, 1455 E 6th Str., Cleveland, OH 44114, USA. *Email address*: damjan.pfajfar@clev.frb.org (D. Pfajfar).

$$\tilde{L}_{ct} = \tilde{\mathcal{U}}_t^{-\sigma_c} + \tilde{\nu}_t(h)\gamma_h \left(\frac{\tilde{c}_t - h\frac{\tilde{c}_{t-1}}{\gamma_t}}{\tilde{X}_{t-1}(h)/\gamma_t} \right)^{\gamma_h - 1} + \tilde{\nu}_t(l)\gamma_l \left(\frac{\tilde{c}_t - h\frac{\tilde{c}_{t-1}}{\gamma_t}}{\tilde{X}_{t-1}(l)/\gamma_t} \right)^{\gamma_l - 1} \tag{A.9}$$

$$\tilde{V}_{ct} = \tilde{L}_{ct} - h\beta E_t \gamma_{t+1}^{-\sigma_c} \tilde{L}_{c,t+1} \tag{A.10}$$

$$\tilde{V}_{ht} = \tilde{\mathcal{U}}_t^{-\sigma_c} \chi_{lt} (1-\alpha_h)(1-H_t)^{(1-\alpha_h)(1-\psi_l)-1} \tilde{X}_t(l) \tag{A.11}$$

$$\tilde{V}_{zht} = -\tilde{\mathcal{U}}_t^{-\sigma_c} \chi_{ht} z h_t^{\psi_h} N_t \tilde{X}_t(h) \tag{A.12}$$

$$\tilde{V}_{zht} + \tilde{V}_{ct}\tilde{w}_t N_t = 0 \tag{A.13}$$

$$\tilde{V}_{c,t} = E_t \mu_t^{RP} \tilde{V}_{c,t+1} \frac{R_t}{\gamma_{t+1}^{\sigma_c}} + \chi \tag{A.14}$$

$$\tilde{\Lambda}_{t,t+1} = \beta \frac{\tilde{V}_{c,t+1}}{\tilde{V}_{c,t}} \tag{A.15}$$

$$\tilde{\nu}_t(h) = -\tilde{\mathcal{U}}_t^{-\sigma_c} \chi_{ht} \frac{z h_t^{1+\psi_h}}{1+\psi_h} N_t + \beta(1-\gamma_h) E_t \gamma_{t+1}^{1-\sigma_c} \tilde{\nu}_{t+1}(h) \frac{\tilde{X}_{t+1}(h)}{\tilde{X}_t(h)} \tag{A.16}$$

$$\tilde{\nu}_t(l) = \tilde{\mathcal{U}}_t^{-\sigma_c} \chi_{lt} \frac{(1-H_t)^{(1-\alpha_h)(1-\psi_l)}}{1-\psi_l} + \beta(1-\gamma_l) E_t \gamma_{t+1}^{1-\sigma_c} \tilde{\nu}_{t+1}(l) \frac{\tilde{X}_{t+1}(l)}{\tilde{X}_t(l)} \tag{A.17}$$

$$\tilde{\mu}_t = \frac{\tilde{V}_{ht}}{\tilde{V}_{ct}} \tag{A.18}$$

$$\tilde{\tilde{V}}_t^h = \tilde{w}_t z h_t - \tilde{\Omega}_t + E_t[\gamma_{t+1}^{1-\sigma_c}(1-\delta_{st+1})\tilde{\tilde{V}}_{t+1}^h \tilde{\Lambda}_{t,t+1}] - E_t[\gamma_{t+1}^{1-\sigma_c}(1-\delta_{st+1}) p_{t+1} \tilde{\Lambda}_{t,t+1} \tilde{\tilde{V}}_{t+1}^h] \tag{A.19}$$

$$p_t \tilde{\tilde{V}}_t^h = \Gamma \tilde{\mu}_t - \tilde{b}_t \tag{A.20}$$

$$\tilde{b}_t = \tilde{b} \tag{A.21}$$

Labor Market:

$$m_t = \overline{\sigma}_{m,t} v_t^{1-\sigma_m} s_t^{\sigma_m} \tag{A.22}$$

$$p_t = \frac{m_t}{s_t} \tag{A.23}$$

$$q_t = \frac{m_t}{v_t} \tag{A.24}$$

$$\theta_t = \frac{v_t}{s_t} \tag{A.25}$$

Final Good Producer/Retailer:

$$\hat{\pi}_t = \frac{\gamma_p}{1+\beta\gamma_p}\hat{\pi}_{t-1} + \frac{slope_{pc}}{100}\hat{p}_t^m + \frac{\beta}{1+\beta\gamma_p} E_t \hat{\pi}_{t+1} + \hat{\epsilon}_t^p \tag{A.26}$$

Intermediate Good Producer/Wage:

$$mpk_t = \alpha \frac{\tilde{Y}_t}{\tilde{k}_t} \tag{A.27}$$

$$\tilde{mpl}_t = (1-\alpha)\frac{\tilde{Y}_t}{N_t} \tag{A.28}$$

$$p_t^m mpk_t = r_t^k \tag{A.29}$$

$$\tilde{\Omega}_t = \tilde{\mathcal{U}}_t^{-\sigma_c} \frac{\chi_{ht}\tilde{X}_t(h)}{\tilde{V}_{ct}} \frac{zh_t^{1+\psi_h}}{1+\psi_h} + \tilde{b}_t + (1-\Gamma)\tilde{\mu}_t \tag{A.30}$$

$$\begin{aligned}\hat{\tilde{\epsilon}}_t^{avg} =& \frac{zh}{\tilde{\epsilon}} z\hat{h}_t + \beta(1-\delta_s)\gamma^{1-\sigma_c}\lambda^w E_t[(\widehat{1-\delta_{st+1}}) + (1-\sigma_c)\hat{\gamma}_{t+1} + \hat{\tilde{\Lambda}}_{t,t+1} \\ &+ \gamma_{w\gamma}\hat{\gamma}_t + \gamma_{wp}\hat{\pi}_t - \hat{\pi}_{t+1} - \hat{\gamma}_{t+1} + \hat{\tilde{\epsilon}}_{t+1}^{avg}]\end{aligned} \tag{A.31}$$

$$\begin{aligned}\hat{\tilde{\mu}}_t^{avg} =& \frac{z_h}{\tilde{\mu}} \tilde{z}_{ht} + \tilde{\phi}_\mu E_t\left[qz\hat{z}_{jt+1}(\tilde{w}_{t+1}) + \omega_1 \hat{\tilde{\mu}}_{t+1}^{avg})\right] \\ &- \tilde{\phi}_\mu qz\Xi\tilde{\mu}\frac{\tilde{\mu}}{zh} E_t\left[\hat{\tilde{w}}_t + \gamma_{w\gamma}\hat{\gamma}_t + \gamma_{wp}\hat{\pi}_t - \hat{\pi}_{t+1} - \hat{\gamma}_{t+1} - \hat{\tilde{w}}_{t+1}\right] \\ &+ \tilde{\phi}_\mu E_t[(1-\delta_s)(\widehat{1-\delta_{st+1}}) + qz\hat{q}_{t+1} + \omega_1(1-\sigma_c)\hat{\gamma}_{t+1} + \omega_1\hat{\tilde{\Lambda}}_{t,t+1} \\ &+ \omega_1(\gamma_{w\gamma}\hat{\gamma}_t + \gamma_{wp}\hat{\pi}_t - \hat{\gamma}_{t+1} - \hat{\pi}_{t+1})]\end{aligned} \tag{A.32}$$

$$\hat{\tilde{\chi}}_t^{avg} = (1-\tilde{\chi})(\hat{\tilde{\epsilon}}_t^{avg} - \hat{\tilde{\mu}}_t^{avg}) \tag{A.33}$$

$$\tilde{\kappa}_{vt} = \tilde{J}_t \tilde{q}_t \tag{A.34}$$

$$\tilde{\kappa}_{vt} = \kappa_1 q_t^{1+\psi_1} z_t^{\psi_1} + \kappa_2 z_t^{\psi_2} \tag{A.35}$$

$$\tilde{\kappa_{nt}} = \kappa_1 \frac{\psi_1}{1+\psi_1} q_t^{1+\psi_1} z_t^{1+\psi_1} + \kappa_2 \frac{\psi_2}{1+\psi_2} z_t^{1+\psi_2} \tag{A.36}$$

$$\tilde{J}_t = p_t^m \tilde{mpl}_t - \tilde{w}_t zh_t + E_t[\gamma_{t+1}^{1-\sigma_c}\tilde{\Lambda}_{t,t+1}\tilde{\kappa}_{nt+1}] + E_t[\gamma_{t+1}^{1-\sigma_c}\tilde{\Lambda}_{t,t+1}(1-\delta_{st+1})\tilde{J}_{t+1}] \tag{A.37}$$

$$\begin{aligned}\hat{\tilde{w}}_t^0(\tilde{w}_t) =& \tilde{\phi}_a\left(\hat{\tilde{p}}_t^m + \hat{\tilde{mpl}}_t\right) + (\tilde{\phi}_s + \tilde{\phi}_x)E_t\left[(1-\sigma_c)\hat{\gamma}_{t+1} + \hat{\tilde{\Lambda}}_{t,t+1}\right] \\ &+ \tilde{\phi}_x\hat{\tilde{\kappa}}_{nt+1}(\tilde{w}_{t+1}) + \tilde{\phi}_s\hat{\tilde{\kappa}}_{vt+1}(\tilde{w}_{t+1}) \\ &+ \tilde{\phi}_b\hat{\tilde{\Omega}}_t + \tilde{\phi}_s E_t\left[\hat{p}_{t+1} + (\widehat{1-\delta_{st+1}}) - \hat{q}_{t+1}\right] \\ &+ \tilde{\phi}_\chi\left[\hat{\chi}_{t,t}^{avg} - \beta\gamma^{1-\sigma_c}\left((1-\delta_s) - p(1-\delta_s)\right)E_t\hat{\chi}_{t+1,t+1}^{avg}\right] \\ &+ \left[\tilde{\phi}_s(1-\eta)^{-1}\rho^n + \tilde{\phi}_\chi(1-\tilde{\chi})(1-\eta)^{-1} - \tilde{\phi}_\chi\beta\gamma^{1-\sigma_c}(1-\delta_s)(1-\tilde{\chi})(1-\eta)^{-1}\rho^n\right]\hat{\eta}_t \\ &- \hat{z}_{ht}\end{aligned} \tag{A.38}$$

$$\begin{aligned}\hat{\tilde{w}}_t =& \gamma_0\hat{\tilde{w}}_t^0 + \gamma_b\left(\hat{\tilde{w}}_{t-1} - \hat{\gamma}_t - \hat{\pi}_t + \gamma_{w\gamma}\hat{\gamma}_{t-1} + \gamma_{wp}\hat{\pi}_{t-1}\right) \\ &+ \gamma_f E_t\left(\hat{\tilde{w}}_{t+1} + \hat{\gamma}_{t+1} + \hat{\pi}_{t+1} - \gamma_{w\gamma}\hat{\gamma}_t - \gamma_{wp}\hat{\pi}_t\right)\end{aligned} \tag{A.39}$$

$$z_t = \frac{v_t}{N_{t-1}} \tag{A.40}$$

Capital Producers and Capital Utilization:

$$\tilde{K}_t = (1-\delta_{k,t})\tilde{K}_{t-1}/\gamma_t + \mu_t^I \tilde{I}_t \left(1 - \frac{\gamma_k}{2}\left(\gamma_t \tilde{I}_t/\tilde{I}_{t-1} - \gamma\right)^2\right) \tag{A.41}$$

$$\delta_{k,t} = \delta_k \tag{A.42}$$

$$a_t = \iota_{u,0}\left[e^{\iota_{u,1}\left(u_t^k - 1\right)} - 1\right] \tag{A.43}$$

$$R_t^k = \frac{u_t^k r_t^k - a_t + (1-\delta_{k,t})q_t^k}{q_{t-1}^k} \tag{A.44}$$

$$q_t^k \mu_t^I \left(1 - \frac{\gamma_k}{2}\left(\gamma_t \tilde{I}_t/\tilde{I}_{t-1} - \gamma\right)^2 - \frac{\gamma_t \tilde{I}_t}{\tilde{I}_{t-1}}\gamma_k \left(\gamma_t \tilde{I}_t/\tilde{I}_{t-1} - \gamma\right)\right) = \tag{A.45}$$

$$1 - E_t \frac{1}{\gamma_{t+1}^{\sigma_c}} \tilde{\Lambda}_{t,t+1} q_{t+1}^k \mu_{t+1}^I \left(\frac{\gamma_{t+1}\tilde{I}_{t+1}}{\tilde{I}_t}\right)^2 \gamma_k \left(\frac{\gamma_{t+1}\tilde{I}_{t+1}}{\tilde{I}_t} - \gamma\right)$$

$$r_t^k = \iota_{u,0}\iota_{u,1} e^{\iota_{u,1}\left(u_t^k - 1\right)} \tag{A.46}$$

Entrepreneurs:

$$\hat{z}_{\omega t} = \frac{log(\bar{\omega}_t) + 0.5\sigma_{\omega,t-1}^2}{\sigma_{\omega,t-1}} \tag{A.47}$$

$$\hat{G}_t = \Phi\left(\hat{z}_{\omega t} - \sigma_{\omega,t-1}\right) \tag{A.48}$$

$$\hat{G}_t' = \bar{\omega}_t \hat{f}_{t-1}\left(\bar{\omega}_t\right) \tag{A.49}$$

$$\hat{\Gamma}_t = \Phi\left(\hat{z}_{\omega t} - \sigma_{\omega,t-1}\right) + \bar{\omega}_t\left[1 - \Phi\left(\hat{z}_{\omega t}\right)\right] \tag{A.50}$$

$$\hat{\Gamma}_t' = 1 - \Phi(\hat{z}_{\omega,t}) \tag{A.51}$$

$$\left\{\hat{\Gamma}_{t+1} - \hat{\mu}\hat{G}_{t+1}\right\}\frac{R_{t+1}^k}{\mu_t^{RP} R_t} - \frac{(\phi_t - 1)}{\phi_t} = 0 \tag{A.52}$$

$$E_t \left\{\left[1 - \hat{\Gamma}_{t+1}\right]\frac{R_{t+1}^k}{\mu_t^{RP} R_t} + \frac{\hat{\Gamma}_{t+1}'\left(\left[\hat{\Gamma}_{t+1} - \hat{\mu}\hat{G}_{t+1}\right]\frac{R_{t+1}^k}{\mu_t^{RP} R_t} - 1\right)}{\hat{\Gamma}_{t+1}' - \hat{\mu}\hat{G}_{t+1}'}\right\} = 0 \tag{A.53}$$

$$\tilde{NW}_t = \hat{\gamma}\left\{\phi_{t-1}\left[\left(1 - \hat{\mu}\hat{G}_t\right)R_t^k - \mu_{t-1}^{RP} R_{t-1}\right] + \mu_{t-1}^{RP} R_{t-1}\right\}\tilde{NW}_{t-1}/\gamma_t + \tilde{W}_t^e \tag{A.54}$$

$$\tilde{K}_t = \frac{\phi_t \tilde{NW}_t}{q_t^k} \tag{A.55}$$

$$default_t = \Phi(\hat{z}_{\omega t}) \tag{A.56}$$

$$spread_t = E_t[R_{t+1}^k] - R_t \tag{A.57}$$

Monetary Policy and Fisher equation:

$$i_t = i_{t-1}^{\rho_i} \left[R\pi \left(\frac{\pi_t}{\pi_t^\star} \right)^{\kappa_\pi} \left(\frac{\tilde{Y}_t}{\tilde{Y}_t^f} \right)^{\kappa_y} \left(\frac{\tilde{Y}_t/\tilde{Y}_t^f}{\tilde{Y}_{t-1}/\tilde{Y}_{t-1}^f} \right)^{\kappa_{gy}} \right]^{(1-\rho_i)} \mu_t^m \tag{A.58}$$

$$hours\_gap_t = \left[\frac{u_t^k}{u_t^{kf}} \right]^\alpha \left[\frac{zh_t N_t}{zh_t^f N_t^f} \right]^{1-\alpha} \tag{A.59}$$

$$R_t = \frac{i_t}{E_t \pi_{t+1}} \tag{A.60}$$

Market Clearing:

$$\begin{aligned} \tilde{Y}_t =& \tilde{c}_t + \tilde{I}_t + \frac{\kappa_1}{1+\psi_1} \left(\frac{q_t v_t}{N_{t-1}} \right)^{1+\psi_1} N_{t-1} + \frac{\kappa_2}{1+\psi_2} \left(\frac{v_t}{N_{t-1}} \right)^{1+\psi_2} N_{t-1} \\ &+ (1 - 1/\widetilde{Gov_t})\widetilde{GDP_t} + a_t \frac{\tilde{K}_{t-1}}{\gamma_t} + \widetilde{FixCost} \end{aligned} \tag{A.61}$$

$$\tilde{Y}_t = \left(\tilde{k}_t \right)^\alpha \left(\gamma_t^{temp} N_t z h_t \right)^{1-\alpha} \tag{A.62}$$

$$\tilde{k}_t = u_t^k \frac{\tilde{K}_{t-1}}{\gamma_t} \tag{A.63}$$

$$\widetilde{GDP}_t = \widetilde{Y}_t \tag{A.64}$$

There are 12 exogenous shock processes,

$$\chi_{lt}, \chi_{ht}, \mu_t^{RP}, \sigma_{\omega t}, \mu_t^I, \tilde{Gov}_t, \sigma_{m,t}, \eta_t, \epsilon_t^p, \gamma_t, \gamma_t^{temp}, \mu_t^m$$

and 12 equations for them:

$$\log \chi_{l,t} = (1 - \rho_{\chi_1} - \rho_{\chi_2}) \log \chi_l + \rho_{\chi_1} \log \chi_{l,t-1} + \rho_{\chi_2} \log \chi_{l,t-2} + \varepsilon_{\chi_l,t}/100$$

$$\log \chi_{h,t} = (1 - \rho_{\chi_h}) \log \chi_h + \rho_{\chi_h} \log \chi_{h,t-1} + \varepsilon_{\chi_h,t}/100$$

$$\log \mu_t^{RP} = (1 - \rho_{RP}) \log \mu^{RP} + \rho_{RP} \log \mu_{t-1}^{RP} + \varepsilon_{RP,t}/100$$

$$\log(\sigma_{\omega,t}) = (1 - \rho_{\sigma_\omega}) \log(\sigma_\omega) + \rho_{\sigma_\omega} \log(\sigma_{\omega,t-1}) + \varepsilon_{\sigma_\omega,t}/100$$

$$\log \mu_t^I = \left(1 - \rho_{\mu^I}\right) \log \mu^I + \rho_{\mu^I} \log \mu_{t-1}^I + \varepsilon_{\mu^I}/100$$

$$\log \widetilde{Gov}_t = (1 - \rho_G) \log \widetilde{Gov} + \rho_G \log \widetilde{Gov}_{t-1} + \varepsilon_{Gov,t}/100 + \theta_{Ga} \varepsilon_{\gamma,t}/100$$

$$\log \overline{\sigma}_{m,t} = (1 - \rho_{\sigma_m}) \log \overline{\sigma}_m + \rho_{\sigma_m} \log \overline{\sigma}_{m,t-1} + \varepsilon_{\sigma_m}/100$$

$$\log \eta_t = (1 - \rho_\eta) \log \eta + \rho_\eta \log \eta_{t-1} + \varepsilon_\eta/100$$

$$\hat{\epsilon}_t^p = \rho_\epsilon \hat{\epsilon}_{t-1}^p + \varepsilon_{\epsilon,t}/100 - \theta_\epsilon \varepsilon_{\epsilon,t-1}/100$$

$$\log \gamma_t = (1 - \rho_\gamma) \log \gamma + \rho_\gamma \log \gamma_{t-1} + \varepsilon_{\gamma,t}/100$$

$$\log \frac{\gamma_t^{temp}}{\gamma^{temp}} = \rho_{\gamma^{temp}} \log \frac{\gamma_{t-1}^{temp}}{\gamma^{temp}} + \varepsilon_{\gamma^{temp},t}/100 - \theta_\gamma \varepsilon_{\gamma^{temp},t-1}/100$$

$$\log \mu_t^m = (1-\rho_m)\log(\mu^m) + \rho_m \log \mu_{t-1}^m + \varepsilon_{m,t}/100$$

A.2 Summary of Equations for the Flexible Economy

Note that in the flexible economy, retailers and firms can optimally set prices and wages each period. All of the exogenous processes and parameter values are the same as in the rigid economy except that the bargaining power shocks and markup shocks do not affect the flexible economy. Also, η in the flexible economy is calibrated to be the same as χ in the rigid economy so both the rigid economy and the flexible economy share the same steady state. The flexible economy has 57 endogenous variables, which are the same as in the rigid economy except for $\pi_t, \tilde{\epsilon}_{t,t}^{avg}, \tilde{\mu}_{t,t}^{avg}, \tilde{\chi}_{t,t}^{avg}, \tilde{w}_t^0, i_t, hours\_gap_t$. The 57 corresponding equations are:

Households:

$$N_t^f = (1-\delta_{st})N_{t-1}^f + p_t^f s_t^f \tag{A.65}$$

$$\tilde{X}_t^f(h) = \left(\tilde{c}_t^f - h\tilde{c}_{t-1}^f/\gamma_t\right)^{\gamma_h} \left(\tilde{X}_{t-1}^f(h)/\gamma_t\right)^{1-\gamma_h} \tag{A.66}$$

$$\tilde{X}_t^f(l) = \left(\tilde{c}_t^f - h\tilde{c}_{t-1}^f/\gamma_t\right)^{\gamma_l} \left(\tilde{X}_{t-1}^f(l)/\gamma_t\right))^{1-\gamma_l} \tag{A.67}$$

$$L_t^f = N_t^f + U_t^f \tag{A.68}$$

$$H_t^f = N_t^f + \Gamma U_t^f \tag{A.69}$$

$$L_t^f = s_t^f + (1-\delta_{st})N_{t-1}^f \tag{A.70}$$

$$u_t^f = \frac{U_t^f}{L_t^f} \tag{A.71}$$

$$\tilde{\mathcal{U}}_t^f = \tilde{c}_t^f - h\frac{\tilde{c}_{t-1}^f}{\gamma_t} + \chi_{lt}\frac{(1-H_t^f)^{(1-\alpha_h)(1-\psi_l)}}{1-\psi_l}\tilde{X}_t^f(l) - \chi_{ht}\frac{zh_t^{f^{1+\psi_h}}}{1+\psi_h}N_t^f\tilde{X}_t^f(h) \tag{A.72}$$

$$\tilde{L}_{ct}^f = \tilde{\mathcal{U}}_t^{f^{-\sigma_c}} + \tilde{\nu}_t^f(h)\gamma_h\left(\frac{\tilde{c}_t^f - h\frac{\tilde{c}_{t-1}^f}{\gamma_t}}{\tilde{X}_{t-1}^f(h)/\gamma_t}\right)^{\gamma_h-1} + \tilde{\nu}_t^f(l)\gamma_l\left(\frac{\tilde{c}_t^f - h\frac{\tilde{c}_{t-1}^f}{\gamma_t}}{\tilde{X}_{t-1}^f(l)/\gamma_t}\right)^{\gamma_l-1} \tag{A.73}$$

$$\tilde{V}_{ct}^f = \tilde{L}_{ct}^f - h\beta E_t\gamma_{t+1}^{-\sigma_c}\tilde{L}_{c,t+1}^f \tag{A.74}$$

$$\tilde{V}_{ht}^f = \tilde{\mathcal{U}}_t^{f^{-\sigma_c}}\chi_{lt}(1-\alpha_h)(1-H_t^f)^{(1-\alpha_h)+(1-\psi_l)-1}\tilde{X}_t^f(l) \tag{A.75}$$

$$\tilde{V}_{zht}^f = -\tilde{\mathcal{U}}_t^{f^{-\sigma_c}}\chi_{ht}zh_t^{f^{\psi_h}}N_t^f\tilde{X}_t^f(h) \tag{A.76}$$

$$\tilde{V}_{zht}^f + \tilde{V}_{ct}^f\tilde{w}_t^f N_t^f = 0 \tag{A.77}$$

$$\tilde{V}_{c,t}^f = E_t\frac{\mu_t^{RP}R_t^f}{\gamma_{t+1}^{\sigma_c}}\tilde{V}_{c,t+1}^f + \chi \tag{A.78}$$

$$\tilde{\Lambda}_{t,t+1}^f = \beta\frac{\tilde{V}_{c,t+1}^f}{\tilde{V}_{c,t}^f} \tag{A.79}$$

$$\tilde{\nu}_t^f(h) = -\tilde{\mathcal{U}}_t^{f^{-\sigma_c}} \chi_{ht} \frac{zh_t^{f^{1+\psi_h}}}{1+\psi_h} N_t^f + \beta(1-\gamma_h) E_t \gamma_{t+1}^{1-\sigma_c} \tilde{\nu}_{t+1}^f(h) \frac{\tilde{X}_{t+1}^f(h)}{\tilde{X}_t^f(h)} \tag{A.80}$$

$$\tilde{\nu}_t^f(l) = \tilde{\mathcal{U}}_t^{f^{-\sigma_c}} \chi_{lt} \frac{(1-H_t^f)^{(1-\alpha_h)(1-\psi_l)}}{1-\psi_l} + \beta(1-\gamma_l) E_t \gamma_{t+1}^{1-\sigma_c} \tilde{\nu}_{t+1}^f(l) \frac{\tilde{X}_{t+1}^f(l)}{\tilde{X}_t^f(l)} \tag{A.81}$$

$$\tilde{\mu}_t^f = \frac{\tilde{V}_{ht}^f}{\tilde{V}_{ct}^f} \tag{A.82}$$

$$\tilde{\tilde{V}}_t^{h^f} = \tilde{w}_t^f z h_t^f - \tilde{\Omega}_t^f + E_t[\gamma_{t+1}^{1-\sigma_c}(1-\delta_{st+1})\tilde{\tilde{V}}_{t+1}^{h^f} \tilde{\Lambda}_{t,t+1}^f] - E_t[\gamma_{t+1}^{1-\sigma_c}(1-\delta_{st+1}) p_{t+1}^f \tilde{\Lambda}_{t,t+1}^f \tilde{\tilde{V}}_{t+1}^{h^f}] \tag{A.83}$$

$$p_t^f \tilde{\tilde{V}}_t^{h^f} = \Gamma \tilde{\mu}_t^f - \tilde{b}_t^f \tag{A.84}$$

$$\tilde{b}_t^f = \tilde{b}^f \tag{A.85}$$

Labor Market:

$$m_t^f = \overline{\sigma}_{m,t} v_t^{f^{1-\sigma_m}} s_t^{f^{\sigma_m}} \tag{A.86}$$

$$p_t^f = \frac{m_t^f}{s_t^f} \tag{A.87}$$

$$q_t^f = \frac{m_t^f}{v_t^f} \tag{A.88}$$

$$\theta_t^f = \frac{v_t^f}{s_t^f} \tag{A.89}$$

Final Good Producer/Retailer:

$$p_t^{mf} = \frac{\Theta - 1}{\Theta} \tag{A.90}$$

Intermediate Good Producer/Wage:

$$mpk_t^f = \alpha \frac{\tilde{Y}_t^f}{\tilde{k}_t^f} \tag{A.91}$$

$$\tilde{mpl}_t^f = (1-\alpha) \frac{\tilde{Y}_t^f}{N_t^f} \tag{A.92}$$

$$p_t^m mpk_t^f = r_t^{fk} \tag{A.93}$$

$$\tilde{\Omega}_t^f = \tilde{\mathcal{U}}_t^{f^{-\sigma_c}} \frac{\chi_{ht} \tilde{X}_t^f(h)}{\tilde{V}_{ct}^f} \frac{zh_t^{f^{1+\psi_h}}}{1+\psi_h} + \tilde{b}_t^f + (1-\Gamma)\tilde{\mu}_t^f \tag{A.94}$$

$$\tilde{\kappa}_{vt}^f = \tilde{J}_t^f \tilde{q}_t^f \tag{A.95}$$

$$\tilde{\kappa}_{vt}^f = \kappa_1 q_t^{f^{1+\psi_1}} z_t^{f^{\psi_1}} + \kappa_2 z_t^{f^{\psi_2}} \tag{A.96}$$

$$\tilde{\kappa}_{nt}^f = \kappa_1 \frac{\psi_1}{1+\psi_1} q_t^{f^{1+\psi_1}} z_t^{f^{1+\psi_1}} + \kappa_2 \frac{\psi_2}{1+\psi_2} z_t^{f^{1+\psi_2}} \tag{A.97}$$

$$\tilde{J}^f_t = p^{fm}_t \tilde{mpl}^f_t - \tilde{w}^f_t zh^f_t + E_t[\gamma^{1-\sigma_c}_{t+1}\tilde{\Lambda}^f_{t,t+1}\tilde{\kappa}^f_{nt+1}] + E_t[\gamma^{1-\sigma_c}_{t+1}\tilde{\Lambda}^f_{t,t+1}(1-\delta_{st+1})\tilde{J}^f_{t+1}] \tag{A.98}$$

$$\begin{aligned}\hat{\tilde{w}}^f_t =& \tilde{\phi}_a\left(\hat{\tilde{p}}^{mf}_t + \hat{\tilde{mpl}}^f_t\right) + (\tilde{\phi}_s + \tilde{\phi}_x)E_t\left[(1-\sigma_c)\hat{\gamma}_{t+1} + \hat{\tilde{\Lambda}}^f_{t,t+1}\right] + \tilde{\phi}_x E_t\hat{\tilde{\kappa}}^f_{nt+1} + \tilde{\phi}_s E_t\hat{\tilde{\kappa}}^f_{vt+1}\\ &+ \tilde{\phi}_b\hat{\tilde{\Omega}}^f_t + \tilde{\phi}_s E_t\left(\hat{p}^f_{t+1} + (1\widehat{-\delta_{st+1}}) - \hat{q}^f_{t+1}\right) - \hat{z}^f_{ht}\end{aligned} \tag{A.99}$$

$$z^f_t = \frac{v^f_t}{N^f_{t-1}} \tag{A.100}$$

Capital Producers and Capital Utilization:

$$\tilde{K}^f_t = (1-\delta^f_{k,t})\tilde{K}^f_{t-1}/\gamma_t + \mu^I_t\tilde{I}^f_t\left(1 - \frac{\gamma_k}{2}\left(\gamma_t\tilde{I}^f_t/\tilde{I}^f_{t-1} - \gamma\right)^2\right) \tag{A.101}$$

$$\delta^f_{k,t} = \delta_k \tag{A.102}$$

$$a^f_t = \iota_{u,0}\left[e^{\iota_{u,1}\left(u^{fk}_t - 1\right)} - 1\right] \tag{A.103}$$

$$R^{fk}_t = \frac{u^{fk}_t r^{fk}_t - a^f_t + (1-\delta^f_{k,t})q^{fk}_t}{q^{fk}_{t-1}} \tag{A.104}$$

$$\begin{aligned}&q^{fk}_t\mu^I_t\left(1 - \frac{\gamma_k}{2}\left(\gamma_t\tilde{I}^f_t/\tilde{I}^f_{t-1} - \gamma\right)^2 - \frac{\gamma_t\tilde{I}^f_t}{\tilde{I}^f_{t-1}}\gamma_k\left(\gamma_t\tilde{I}^f_t/\tilde{I}^f_{t-1} - \gamma\right)\right) =\\ &1 - E_t\frac{1}{\gamma^{\sigma_c}_{t+1}}\tilde{\Lambda}^f_{t,t+1}q^{fk}_{t+1}\mu^I_{t+1}\left(\frac{\gamma_{t+1}\tilde{I}^f_{t+1}}{\tilde{I}^f_t}\right)^2\gamma_k\left(\frac{\gamma_{t+1}\tilde{I}^f_{t+1}}{\tilde{I}^f_t} - \gamma\right)\end{aligned} \tag{A.105}$$

$$r^{fk}_t = \iota_{u,0}\iota_{u,1}e^{\iota_{u,1}\left(u^{fk}_t - 1\right)} \tag{A.106}$$

Entrepreneurs:

$$\hat{z}^f_{\omega t} = \frac{log(\bar{\omega}^f_t) + 0.5\sigma^2_{\omega,t-1}}{\sigma_{\omega,t-1}} \tag{A.107}$$

$$\hat{G}^f_t = \Phi\left(\hat{z}^f_{\omega t} - \sigma_{\omega,t-1}\right) \tag{A.108}$$

$$\hat{G}^{f\prime}_t = \bar{\omega}^f_t\hat{f}_{t-1}\left(\bar{\omega}^f_t\right) \tag{A.109}$$

$$\hat{\Gamma}^f_t = \Phi\left(\hat{z}^f_{\omega t} - \sigma_{\omega,t-1}\right) + \bar{\omega}^f_t\left[1 - \Phi\left(\hat{z}^f_{\omega t}\right)\right] \tag{A.110}$$

$$\hat{\Gamma}^{f\prime}_t = 1 - \Phi(\hat{z}^f_{\omega t}) \tag{A.111}$$

$$\left\{\hat{\Gamma}^f_{t+1} - \hat{\mu}\hat{G}^f_{t+1}\right\}\frac{R^{fk}_{t+1}}{\mu^{RP}_t R^f_t} - \frac{\left(\phi^f_t - 1\right)}{\phi^f_t} = 0 \tag{A.112}$$

$$E_t\left\{\left[1 - \hat{\Gamma}^f_{t+1}\right]\frac{R^{fk}_{t+1}}{\mu^{RP}_t R^f_t} + \frac{\hat{\Gamma}^{f\prime}_{t+1}\left(\left[\hat{\Gamma}^f_{t+1} - \hat{\mu}\hat{G}^f_{t+1}\right]\frac{R^{fk}_{t+1}}{\mu^{RP}_t R^f_t} - 1\right)}{\hat{\Gamma}^{f\prime}_{t+1} - \hat{\mu}\hat{G}^{f\prime}_{t+1}}\right\} = 0 \tag{A.113}$$

$$\tilde{NW}_t^f = \hat{\gamma}\left\{\phi_{t-1}^f\left[\left(1-\hat{\mu}\hat{G}_t^f\right)R_t^{fk} - \mu_{t-1}^{RP}R_{t-1}^f\right] + \mu_{t-1}^{RP}R_{t-1}^f\right\}\tilde{NW}_{t-1}^f/\gamma_t + \tilde{W}_t^e \tag{A.114}$$

$$\tilde{K}_t^f = \frac{\phi_t^f \tilde{NW}_t^f}{q_t^{fk}} \tag{A.115}$$

$$default_t^f = \Phi(\hat{z}_{\omega t}^f) \tag{A.116}$$

$$spread_t^f = E_t[R_{t+1}^{kf}] - R_t^f \tag{A.117}$$

Market Clearing:

$$\begin{aligned}\tilde{Y}_t^f =& \tilde{c}_t^f + \tilde{I}_t^f + \frac{\kappa_1}{1+\psi_1}\left(\frac{q_t^f v_t^f}{N_{t-1}^f}\right)^{1+\psi_1} N_{t-1}^f + \frac{\kappa_2}{1+\psi_2}\left(\frac{v_t^f}{N_{t-1}^f}\right)^{1+\psi_2} N_{t-1}^f \\ &+ (1-1/\tilde{Gov}_t)\tilde{GDP}_t^f + a_t^f\frac{\tilde{K}_{t-1}^f}{\gamma_t} + Fix\tilde{C}ost\end{aligned} \tag{A.118}$$

$$\tilde{Y}_t^f = \left(\tilde{k}_t^f\right)^{\alpha}\left(\gamma_t^{temp}N_t^f zh_t^f\right)^{1-\alpha} \tag{A.119}$$

$$\tilde{k}_t^f = u_t^{fk}\frac{\tilde{K}_{t-1}^f}{\gamma_t} \tag{A.120}$$

$$\widetilde{GDP}_t^f = \tilde{Y}_t^f \tag{A.121}$$

A.3 Parameters

Table A.1: Model Parameters

PARAMETER	*SYMBOL*	*VALUE*
Steady–state job finding rate	p_{ss}	0.83
Matching elasticity with respect to unemployment	σ_m	0.81
Ratio of vacancy posting costs parameters	$\log\kappa_{21}$	-6.49
Hiring–rate cost elasticity	ψ_1	1.53
Vacancy–rate cost elasticity	ψ_2	1.17
SS ratio of outside option to MPL plus hiring cost	Ω_p	0.83
SS ratio of b plus utility cost of employ to outside option	Γ^{Ω}	0.43
SS ratio of b to the participation component of outside option	b^0	0.98
Log of JR parameter for hours	$\log\gamma_h$	-2.56
Log of JR parameter for participation margin	$\log\gamma_l$	-3.29
Inverse employment elasticity	ψ_l	1.86
SS workers' bargaining power	η	0.57
Nominal wage rigidity	λ_w	0.04
Capital depreciation	δ_k	0.025
Capital share	α	0.33

Continued on next page

Table A.1 – continued from previous page

PARAMETER	*SYMBOL*	*VALUE*
Share of government spending in GDP at the steady state	$\frac{Gov_\star}{Y_\star}$	0.20
Share of investment in GDP at the steady state	$\frac{I_\star}{Y_\star}$	0.20
Net inflation at the steady state (quarterly)	$\pi_\star$	0.005
100*Spread at steady state	$100 \cdot \left(R^k - R\right)$	0.5085
Kimball aggregator	Θ	5.19
Job–filling rate at the steady state	$q_\star$	0.95
Survival rate for firms	$\widehat{\gamma}$	0.975
100*Entrepreneurial default rate at steady state	$100 \cdot \widehat{F}\left(\overline{\omega}\right)$	0.56
Constant in the consumption meas. equation	c_{dc}	0.13
Constant in the investment meas. equation	c_{dc}	-0.29
Constant in the comp. per hour meas. equation	c_{dw}	-0.02
Constant in the average hourly earnings meas. equation	c_{ahe}	-0.20
Discount factor	β	0.9934
Intertemporal elast. of substitution	$1/\sigma_c$	1.12
Habit parameter	h	0.38
Capital utilization	$\iota_{u,1}$	0.93
Capital adj. cost	γ_k	5.91
Slope of the Phillips curve	$slope$	1.10
Inflation indexation	γ_p	0.39
Wage indexation to past inflation	γ_{wp}	0.49
Inflation coefficient (Taylor rule)	κ_π	1.48
Output gap coefficient (Taylor rule)	κ_y	0.46
Output gap growth coefficient (Taylor rule)	κ_{yg}	0.32
Taylor rule smoothing	ρ_i	0.70
Fraction of capital diverted	$\widehat{\mu}$	0.12
Endogenous Parameters (at Posterior Mode)		
Steady–state pref parameter extensive margin	χ_l	0.070
Steady–state pref parameter intensive margin	χ_h	0.950
Separation rate	δ_s	0.338
Elasticity of intensive labor supply	ψ_h	1.054
Effort parameter	Γ	0.984
Steady–state matching efficiency	$\bar{\sigma}_m$	0.854
Post-match cost parameter	κ_1	0.855
Pre-match cost parameter	κ_2	0.001

Continued on next page

Table A.1 – continued from previous page

PARAMETER	*SYMBOL*	*VALUE*
Flow opportunity cost of employment relative to productivity	$\Omega/(p^m mpl)$	0.845
Unemployment benefits relative to productivity	$b/(p^m mpl)$	0.359
Steady–state leverage	ϕ_e	4.269
Steady–state entrepreneurial risk	σ_ω	0.105
Steady–state entrepreneurial endowment	W_e	0.001
Fixed cost	Φ	0.055
Scale factor for capital utilization costs	$\iota_{u,0}$	0.043
Shock Autocorrelations		
Convenience yield shock	$\rho_{\mu^{CY}}$	0.93
Participation/home production shock	ρ_{χ_l}	0.98
Preference shock to hours	ρ_{χ_h}	0.92
Matching efficiency shocks	$\rho_{\bar{\sigma}_m}$	0.95
Bargaining power shocks	ρ_η	0.52
Productivity shocks	ρ_γ	0.50
Investment-specific tech. shock	ρ_{μ^I}	0.84
Risk shock	ρ_{σ_ω}	0.50
Monetary policy shock	ρ_m	0.79
Government spending shock	ρ_g	0.95
Other Shock Parameters		
Correlation gov. spending shock – TFP shock	θ_{ga}	-0.41
Factor loading for core PCE inflation	$\Lambda_{\pi,p}$	1.00
Factor loading for average hourly earnings	$\Lambda_{\pi,w}$	0.73
Shock Standard Deviations		
Convenience yield shock	$\sigma_{\mu^{CY}}$	0.20
Participation/home production shock	σ_{χ_l}	0.51
Preference shock to hours	σ_{χ_h}	0.30
Price markup shock	σ_{ϵ^p}	0.05
Matching efficiency shocks	$\sigma_{\bar{\sigma}_m}$	0.65
Bargaining power shocks	σ_η	0.09
Productivity shock	σ_γ	0.15
Investment-specific tech. shock	σ_{μ^I}	1.89
Risk shock	σ_{σ_ω}	0.09
Monetary policy shock	σ_m	0.10

Continued on next page

Table A.1 – continued from previous page

PARAMETER	*SYMBOL*	*VALUE*
Government spending shock	σ_g	0.17
Measurement Error Standard Deviations		
Output growth	$\sigma_{\Delta y}$	0.38
Consumption growth	$\sigma_{\Delta c}$	0.40
Investment growth	$\sigma_{\Delta i}$	0.99
Wage growth: Comp. per employee	$\sigma_{\Delta w}$	0.55
Wage growth: Average weekly earnings	$\sigma_{\Delta AWE}$	0.32
Inflation: GDP deflator	σ_{π}	0.13
Inflation: PCE	σ_{π}	0.11
Unemployment	σ_u	0.03
Participation rate	σ_{lfpr}	0.09
Workweek	σ_{ww}	0.00
Vacancies	σ_{vobs}	0.00

Notes: SS stands for steady state. MPL stands for marginal product of labor.

JR stands for Jaimovich-Rebelo.

A.4 Time-varying Taylor Rule Parameters

Figure A.1: Time-Varying Taylor Rule Parameters

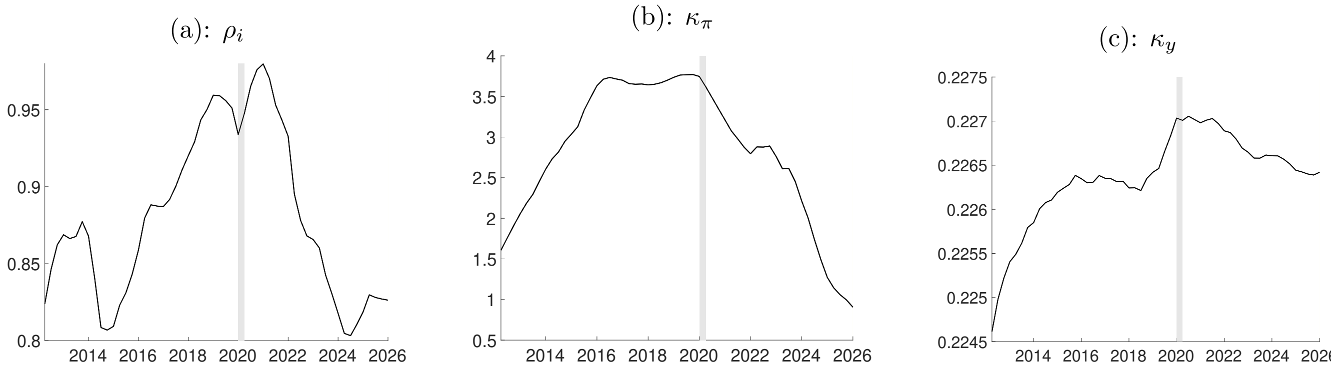

Notes: Shaded areas represent NBER recession dates.

A.5 Expected ELB Duration

During our sample period, the federal funds rate reached the effective zero lower bound (ELB) on two occasions: from January 2009 through December 2015 in the aftermath of the Great Recession, and from March 2020 through February 2022 in the aftermath of the Covid Recession. To generate a series of expected ELB durations for each quarter when the federal funds rate was at the ELB, we employ

Blue Chip data from 2008 through 2010 and the Survey of Primary Dealers starting in January 2011. The expected ELB duration series utilized in this paper is displayed in Figure A.2. Our construction methodology proceeds as follows: For the Blue Chip microdata, we calculate the expected ELB duration (measured in quarters) for each individual forecaster and month, then derive the median across forecasters for each quarter. Although Blue Chip conducts monthly surveys, respondents provide forecasts for the expected federal funds rate at quarterly frequencies. From 2011 onward, we utilize the Survey of Primary Dealers. During the January 2011 to 2015 period, this survey solicits the *"Most Likely Quarter and Year of First Target Rate Increase."* In subsequent periods, it requests the particular FOMC meeting at which the target rate will rise.

Figure A.2: Expected ELB duration

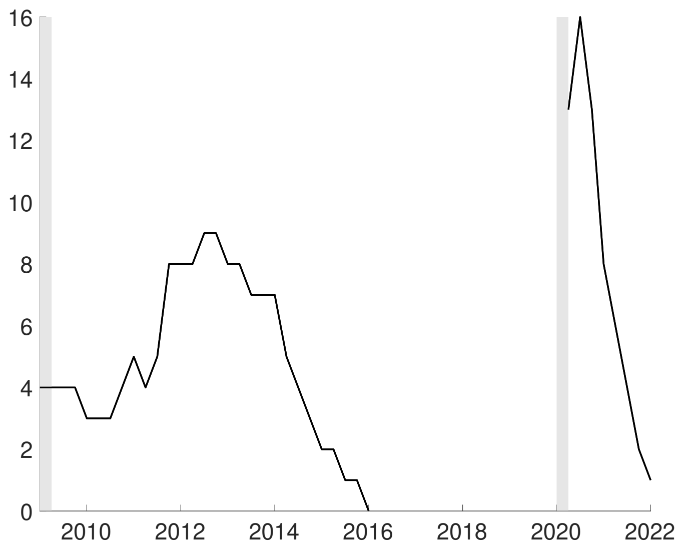

Notes: Y-axis represents number of quarters that the ELB is expected to bind. Shaded regions represent NBER recessions.

B All Labor Market Gaps

Figure A.3: Model-Based Flexible-Price Gaps

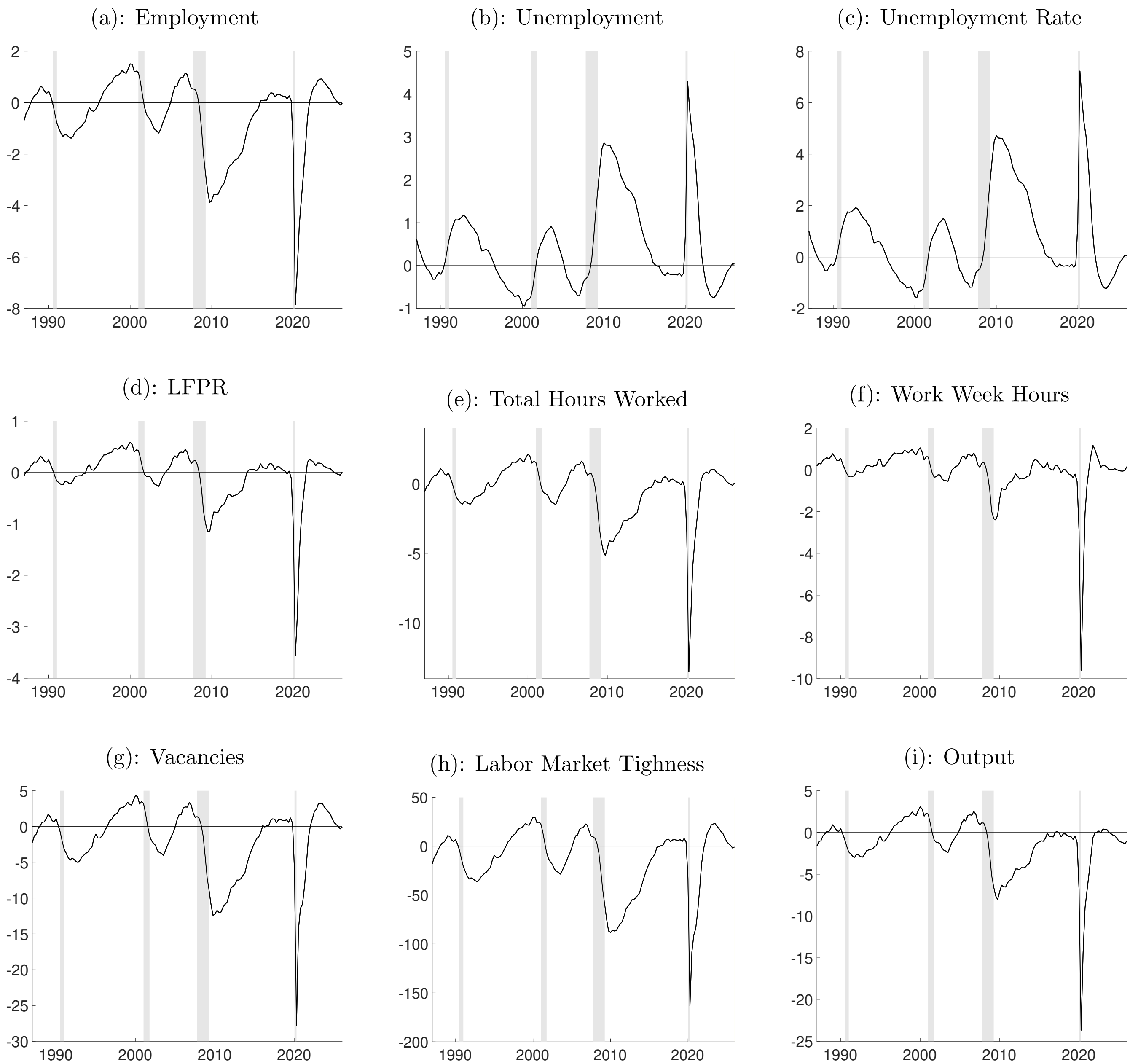

Notes: The figure plots the model-based flexible-price gaps. The horizontal axis represents time and the vertical axis represents percentage point deviations from the flexible-price variable. Shaded areas represent NBER recession dates.

C Okun's Law

Figure A.4: Unemployment Rate Gap vs Output Gap

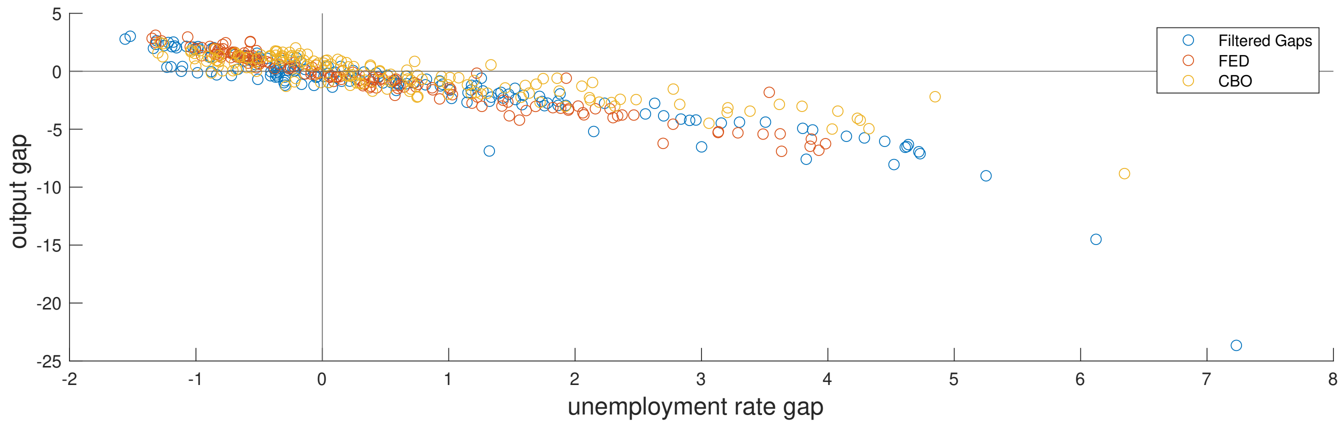

Notes: The x-axis represents the unemployment rate gap, while the y-axis represents the output gap. Blue dots are our estimated gaps, while red and yellow dots represent the estimated gaps by the Federal Reserve and the CBO, respectively.

D Double decomposition

Figure A.5: Double decomposition SLMI